EXPERIMENTAL EVALUATION OF THE ELECTROMAGNETIC CURRENT TRANSDUCER

A THESIS

SUBMITTED TO THE

FACULTY OF GRADUATE STUDIES

THE UNIVERSITY OF MANITOBA

IN PARTIAL FULFILLMENT

OF THE REQUIREMENTS FOR THE DEGREE OF

MASTER OF SCIENCE IN ELECTRICAL ENGINEERING

by M.M. NEY 1977

EXPERIMENTAL EVALUATION OF THE ELECTROMAGNETIC CURRENT TRANSDUCER

BY

MICHEL NEY

A dissertation submitted to the Faculty of Graduate Studies of the University of Manitoba in partial fulfillment of the requirements of the degree of

MASTER OF SCIENCE

ABSTRACT

A new current transducer for the purpose of protection and control of E.H.V.D.C. power systems based on the application of a microwave YIG tuned filter as a basic sensor is described. The sensor behaves like a magnetically tuned microwave resonator whose resonant frequency is proportional to the strength of the magnetic field created by the direct current flowing in the E.H.V. line. A microwave generator located at the ground potential is locked to the resonant frequency of the YIG filter. The principle of operation, description of the system and experimental results obtained in the Laboratory are presented and comparisons are made with the results which have been reported in an earlier thesis on the electronic part of the system. It was found that the concept of the current transducer is technically feasible for monitoring E.H.V.D.C. power systems.

ACKNOWLEDGEMENTS

I would like to thank my supervisor, Professor S.S. Stuchly, for his help and guidance in completing this research. I would like to thank Professor M. Yunik, Professor M.Z. Tarnawecky and Dr. A. Kraszewski for their invaluable help.

I would like to express my appreciation to the Manitoba Research Council for providing the financial support for this work and for the help and assistance by Manitoba Hydro at different stages of this research.

Finally, I would like to thank Mrs. Alix Bernheim for her careful typing of this thesis.

TABLE OF CONTENTS

LIST OF FIGURES

Chapter 1

INTRODUCTION

Two factors will tend to enhance the use of D.C. power transmission in the future. First, the impending shortage of fuels will require greater interconnection of large electrical systems for more efficient use of energy. Secondly, the rapid advances now being made in solid state conversion equipment will make D.C. a more versatile method of transmission, distribution and interconnection.

The comparison between H.V.A.C. and H.V.D.C. has been discussed in many papers [1] [2]. Today, both systems are generally accepted as necessary and reliable.

Power systems are using ever increasing voltages in both A.C. and D.C. transmission networks. In D.C. transmission systems, voltages of ± 800 kV are now a reality and higher voltages are being considered.

In D.C. systems, information regarding the line current is required for operation of regulation and protection devices. Accuracy of the current measurement is very important, especially for control purposes. Accuracy of 1% of the nominal current is required*. Currents greater than one p.u. are expected to last only a very short period and the accuracy of the measuring device for these currents is not as important. The current transducer should have good linearity over the whole range of operation (usually 1.0 to 3.0 p.u. of the nominal current), a wide dynamic range

* Manitoba Hydro requirements

and a fast response, especially when fast acting circuit breakers or control devices (around 2000 A/ms) are used. Finally, the current transducer should operate in ambiant temperatures between -55°C and 60°C.

During the last decade several new A.C. and D.C. current transducers have been suggested. Most of them contain two basic parts : a high potential unit located close to the power line conductor and a low potential unit, usually ground. Transmission of information between the units is realized by either a microwave or optical link. This is achieved by using a free space propagation path through the atmosphere or dielectric waveguides or lightguides. The propagation path provides the necessary electric insulation between the high potential and low potential units.

The majority of the new current transducers make use of the optical Faraday's effect [3]. When a linearly polarized electromagnetic wave passes through a medium magnetized in the direction of propagation, the plane of polarization is rotated. The angle of rotation is proportional to the line integral of the magnetic field along the propagation path in the medium. Optical rays from a monochromatic source at the ground level pass through the sensor itself and are reflected downwards by the reflecting surface. The reflected beam then returns to ground level where it passes through an analyser and finally reaches a detector. The analyser output is proportional to the magnitude of the rotation caused by the Faraday's effect, and hence to the line current. These systems give a good linearity and a fast response time. However, they require a supporting insulator for the laser and other components which make the system expensive.

A D.C. current transducer which is in common use is basically a magnetic amplifier [4]. It consists of two series connected saturable magnetic cores. The direct current to be measured flows through the cores. The secondaries are connected in series opposition and supplied by an auxiliary transformer. The average current in the secondaries is proportional to the current which flows through the power line. The system is characterized by a long response time (approximately 10 ms) and poor insulation, but is stable and insensitive to temperature variations.

The system evaluated in this work also consists of a high potential unit placed at the potential of line and a ground unit. A YIG-tuned filter* is located in the vicinity of the conductor. The filter is fed by a microwave generator placed at ground potential through a dielectric waveguide. A frequency tracking system locks the generator to the resonant frequency of the YIG filter which is linearly dependent on the magnetic field strength. Since the sensor is a passive device, the high potential unit does not require any power for normal operation.

Since the YIG filter is a device which can be used efficiently for measuring the magnetic field surrounding a conductor, a tracking system has been developed to lock a microwave generator onto its resonant frequency to obtain an output voltage signal which is proportional to the magnetic field strength and hence to the current in the line [7].

* The YIG resonator consists of a small, highly polished sphere of single crystal yttrium-iron-garnet. The properties of the YIG crystals and YIG-based devices have been studied and described in considerable details [5] [6].

Excellent results have been reported concerning the dynamic performances of the tracking system [7]. It was found to have a bandwidth of 20 kHz, a rise time of 0.03 ms, and a tracking accuracy of the order of one part in 10^{-5}.

Chapter 2

DESCRIPTION OF THE SYSTEM

2.1 PRINCIPLE OF OPERATION

A block diagram of the current measurement system evaluated in this work is shown in Fig. 2.1. The YIG reflection filter is held in a fixed position (Fig. 2.2) with respect to the transmission line. The resonant frequency of the filter varies proportionally to the strength of the magnetic field surrounding the line. A dielectric waveguide provides the insulation between the high potential and ground unit.

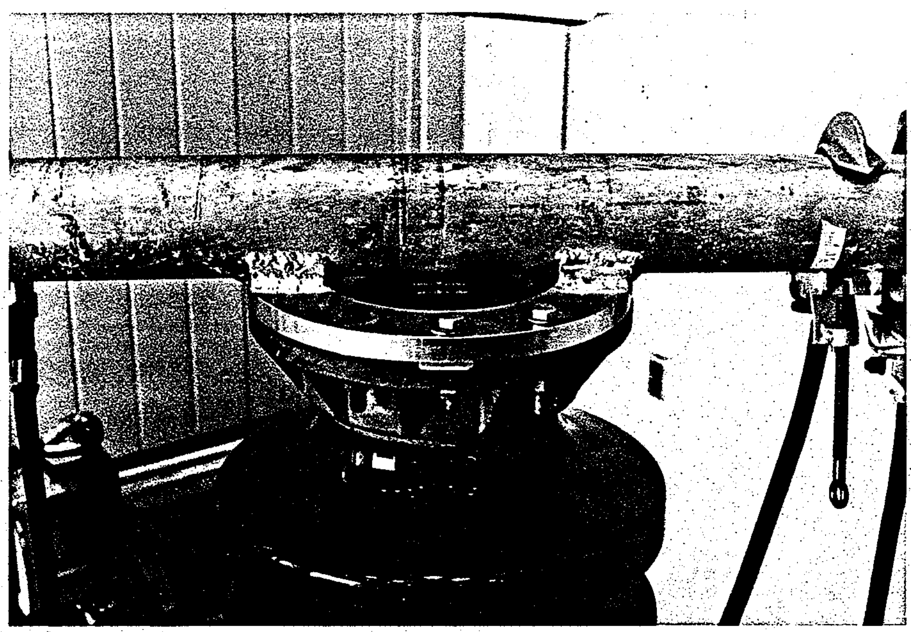

Figure 2.2 : YIG FILTER AND BUS LINE ARRANGEMENT

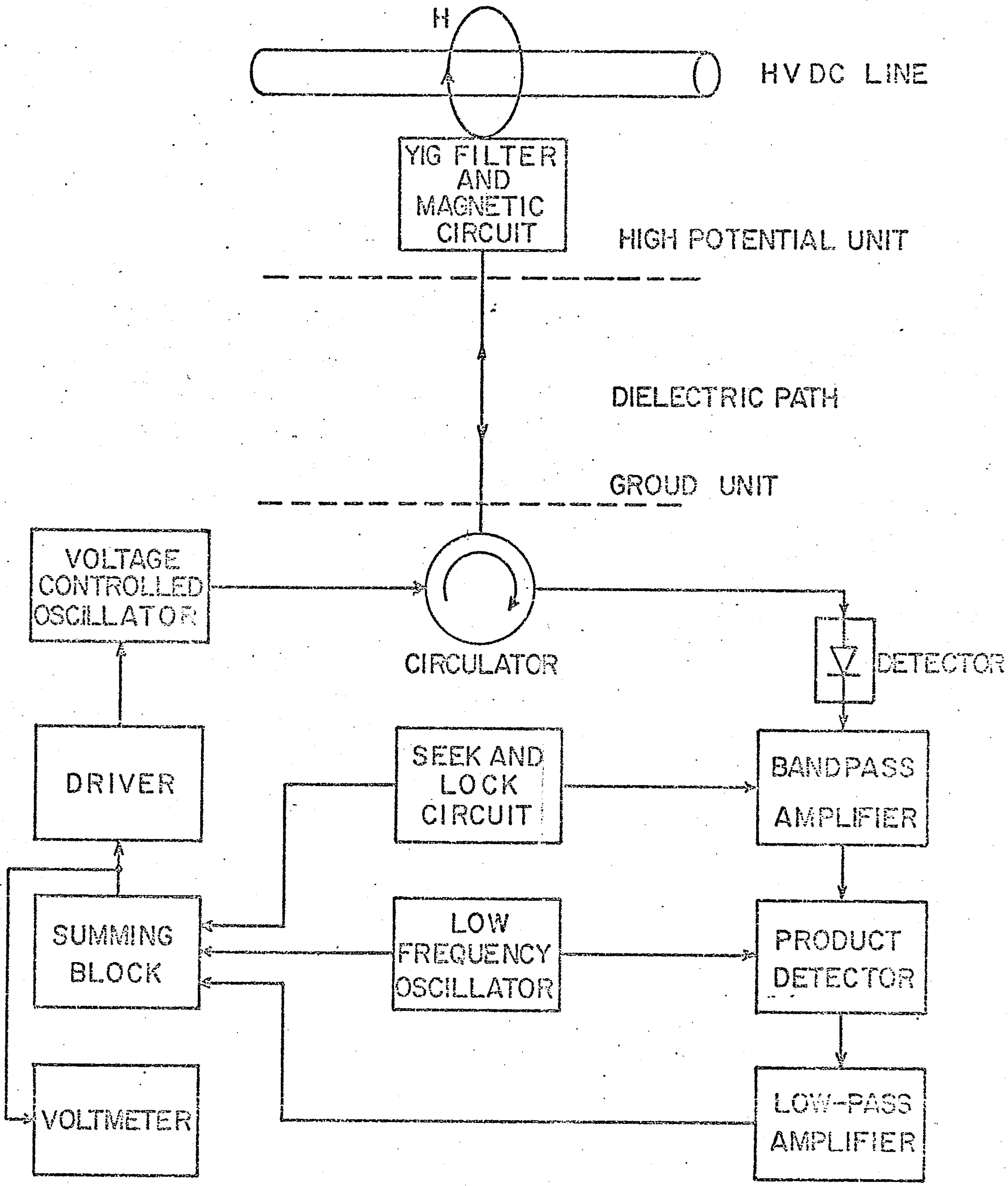

Figure 2.1 : CURRENT MEASUREMENT SYSTEM

The tracking system is located at the ground potential. A low frequency oscillator modulates the voltage controlled oscillator (VCO). A resulting FM signal is fed to the YIG filter through a circulator and the dielectric waveguide, and after reflection returns to an envelope detector. In Fig. 2.3, the detector outputs are shown for VCO frequencies higher than, lower than, and equal to the YIG filter's resonant frequency. For higher VCO frequencies the low frequency oscillator signal and the detector output signal are in phase, while for lower VCO frequencies, they are 180^{o} out of phase. It can be seen that when the VCO is at the YIG filter's resonant frequency, the detector output does not contain the fundamental of the frequency modulation. Therefore, the amplitude of the fundamental, which depends on the slope of the YIG's characteristic, represents the error signal of the tracking loop since its amplitude depends also on the difference between the VCO frequency and the YIG filter's resonant frequency. The fundamental frequency is amplified by a bandpass amplifier and then fed to a product detector whose output contains a D.C. voltage which is positive or negative depending on the relative phase of the input signal and the phase of the low frequency oscillator. The amplitude of this D.C. signal is proportional to the amplitude of the input signal. A lowpass amplifier filters out the higher order mixing products generated by the product detector. A resulting D.C. signal is fed into a summing circuit and then to the VCO where it is used to tune it to the resonant frequency of the YIG filter.

Γ_0 REFLECTION COEFFICIENT AT THE YIG'S RESONANT FREQUENCY

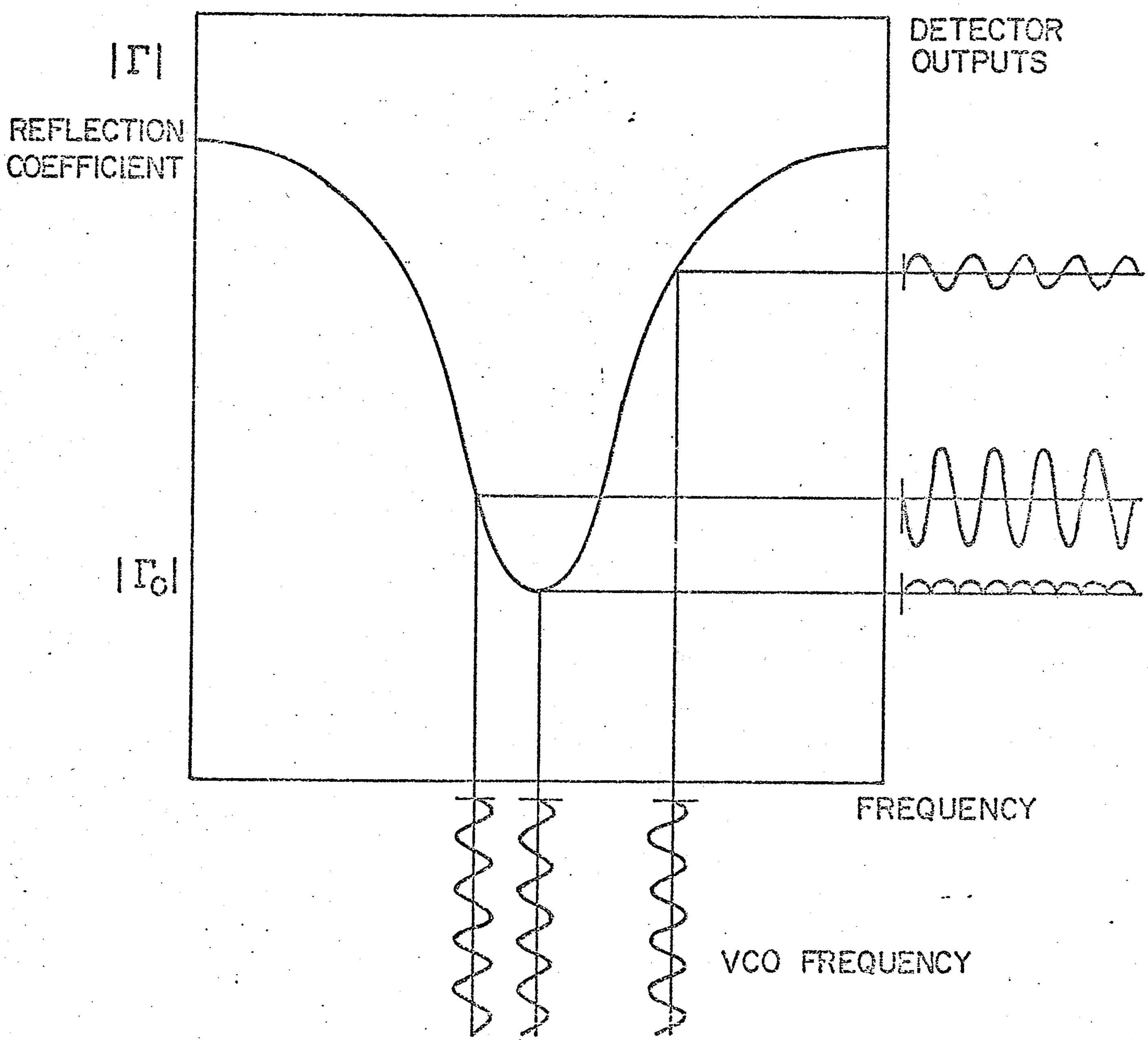

Figure 2.3 : DETECTOR OUTPUT WAVEFORMS

The tracking loop was studied by *MacDonald* [7]. It was found that for small frequency deviations the system behaves in a linear fashion. Also, when the deviation is large, but the rate of change (derivative) is smaller than the slew rate of the tracking loop, the system remains linear.

2.2 *INSTABILITY OF THE SYSTEM*

The system becomes unstable (does not track) in two cases, namely, when large changes of frequency occur, or when the open loop gain is too large. Since the open loop gain is adjustable, the second situation never occurs. When the loop is not able to keep the system tracking, the seek-and-lock circuit short-circuits the output of the bandpass amplifier and makes the VCO sweep over the operating range of frequencies. The output of the detector is then compared with an adjustable reference level (Fig. 2.4). Once the detector output signal becomes smaller than this reference level, and the input signal slower than the slew rate of the system, the seek-and-lock circuit is automatically switched off.

The seek-and-lock circuit also prevents the tracking system from locking the VCO's frequency to any other frequency point other than the filter's resonant frequency.

2.3 *HIGH FREQUENCY OPERATING RANGE*

A frequency of 10.5 GHz was selected as the center operating frequency of the filter. The system is able to track and lock to the YIG filter's resonant frequency in the range from 10 to 11 GHz. A D.C. biasing

Γ_0 REFLECTION COEFFICIENT AT THE YIG'S RESONANT FREQUENCY

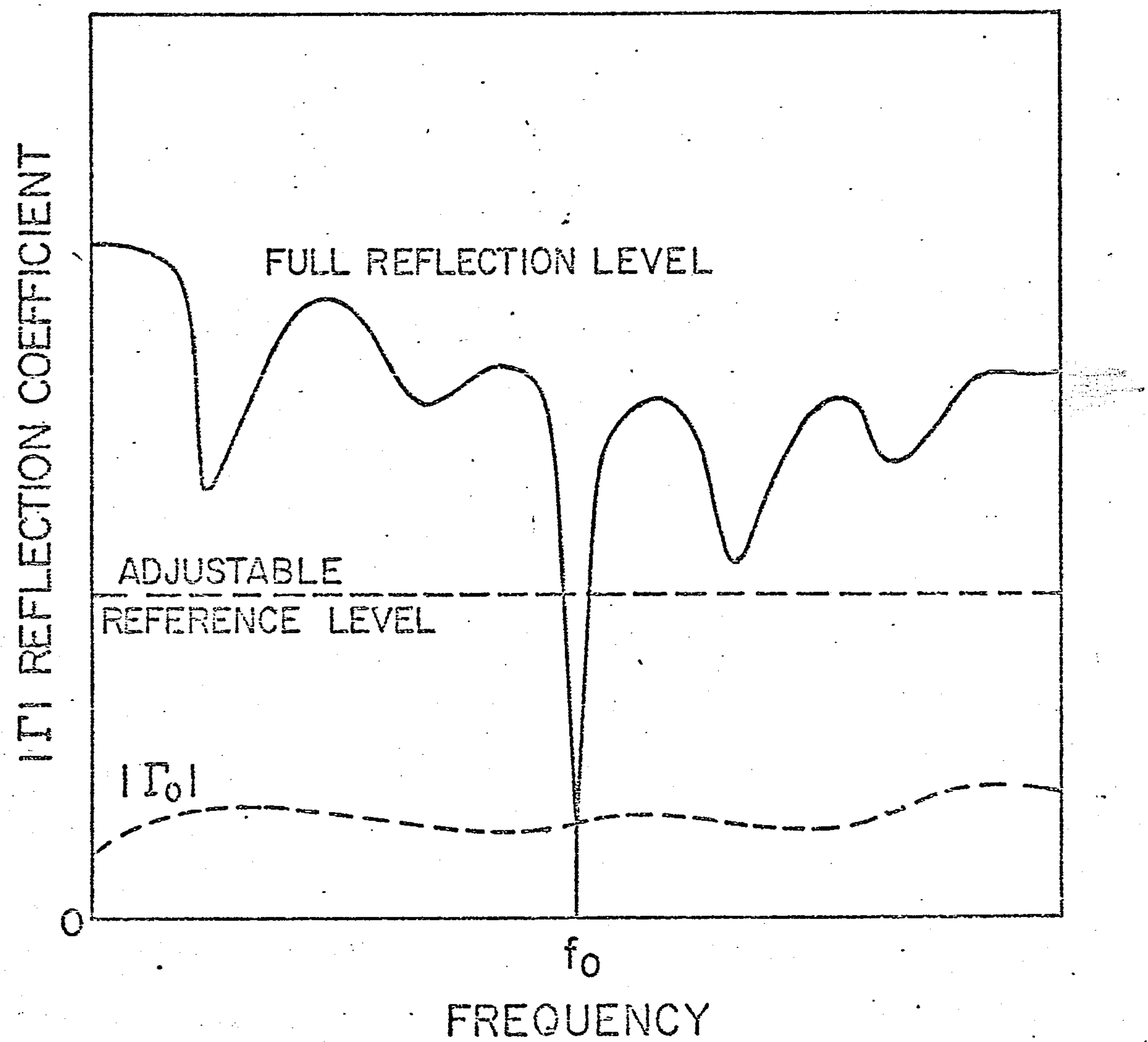

Figure 2.4 : OUTPUT DETECTOR CHARACTERISTIC (Tracking system off)

circuit sets the operating point of the VCO at 10.5 GHz.

A distance of 5.1 m (17 feet) was required between the two units to provide sufficient insulation. Therefore, a dielectric waveguide with a high resistivity was perfectly suited to this requirement. Because of its availability and suitable characteristics, a teflon dielectric rod was chosen. In order to obtain a single propagation mode and minimum losses in the operating frequency range a diameter of 1.8 mm (3/4 inch) was selected. Cylindrical metal launching devices followed by cylindrical-to-rectangular waveguide transitions were installed at both ends of the waveguide. The dielectric waveguide consists of three sections screwed together. The space between the threads was filled with a dielectric resin.

2.4 *BIASING D.C. MAGNETIC CIRCUIT*

In order to have the YIG filter operating in the frequency range from 10 to 11 GHz, a biasing D.C. magnetic circuit was needed. Since no electrical power could be drawn from the D.C. line, permanent magnets were used. A biasing field of about 3.7 kOe was required to set the filter's resonant frequency at 10.5 GHz. Because of the good parameters and temperature stability, Lanthanet LM-18 magnets were chosen. A characteristic of the magnetic circuit e.g. the distance between the magnets vs magnet diameter for the biasing field H_o = 3700 Oe is shown in Fig. 2.5, while Fig. 2.6 shows the derivative of the magnetic field with respect to the distance between the magnets. These characteristics enable evaluation of the variations of the biasing magnetic field resulting from the thermal expansion of the magnets' holder.

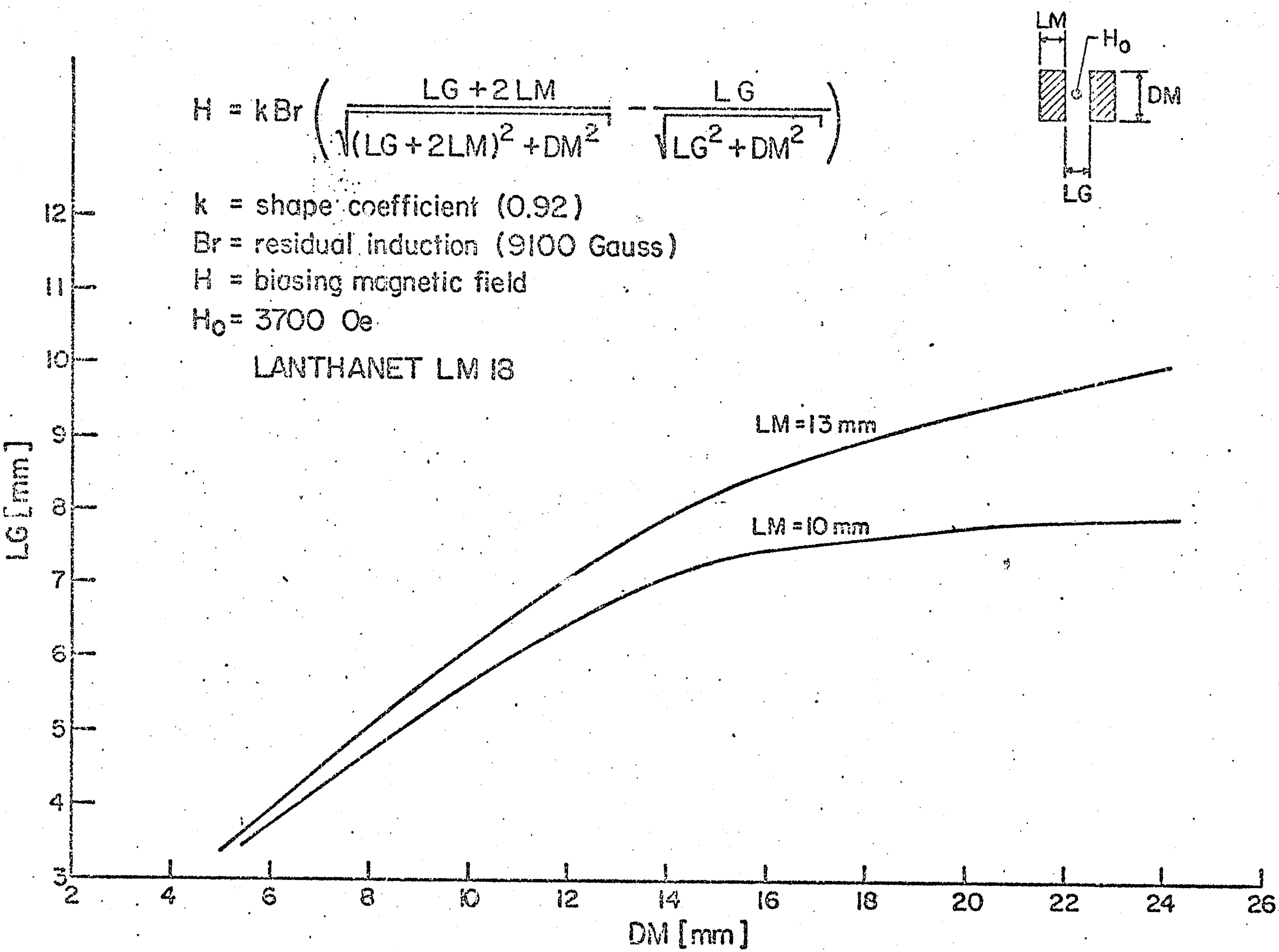

Figure 2.5 : MAGNETIC CIRCUIT CHARACTERISTIC LG = f(DM)

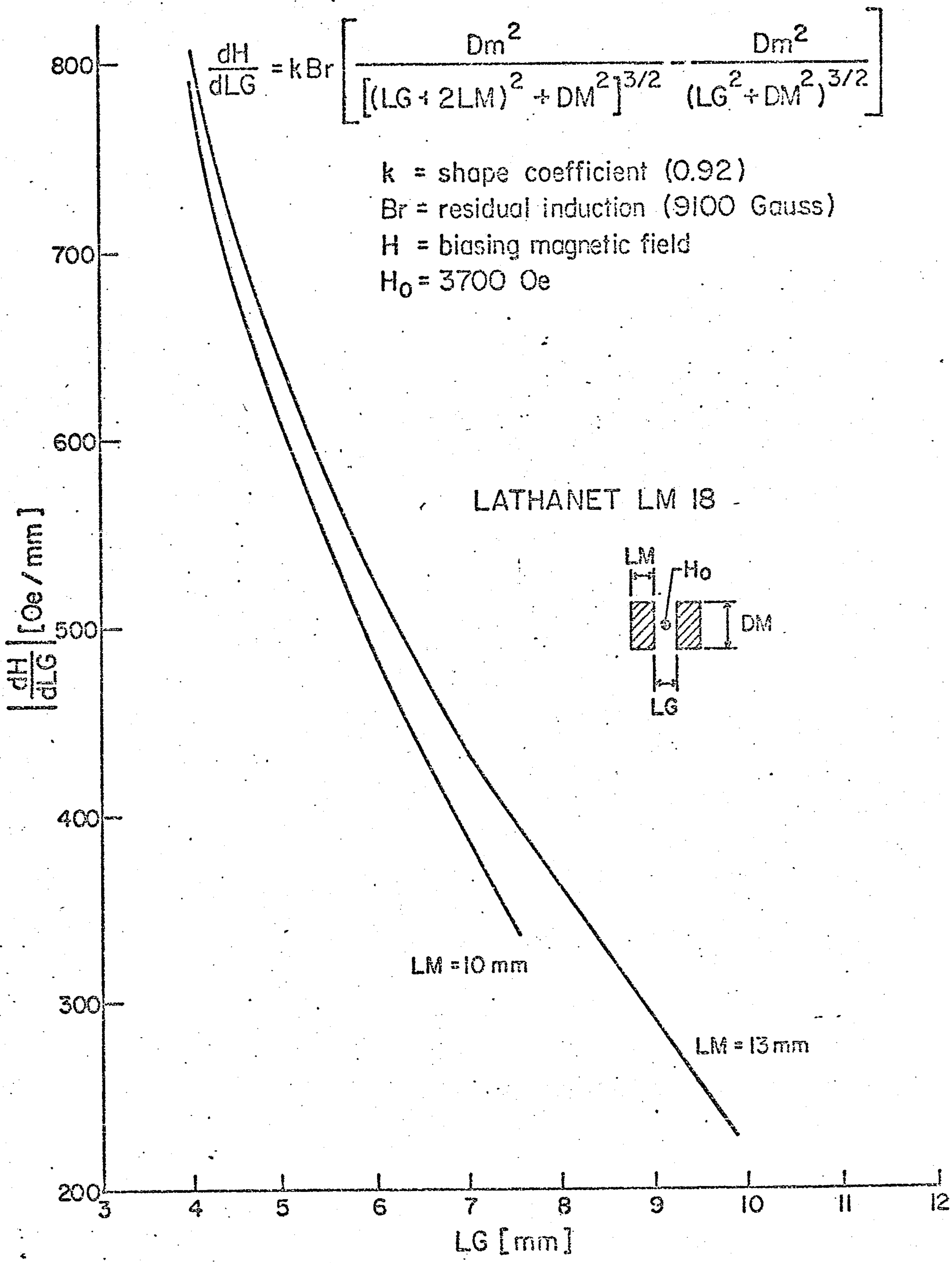

Figure 2.6 : MAGNETIC CIRCUIT CHARACTERISTIC dH/dLG = f(LG)

Chapter 3

EXPERIMENTAL PROCEDURES

3.1 *INTRODUCTION*

Several experiments were conducted to evaluate the performance of the current transducer under simulated operating conditions. Most of the experiments were carried out in the laboratory. A final calibration of the system was done at the Manitoba Hydro Dorsey converter station, using a high D.C. current generator.

The test prototype differed somewhat from the final version, namely, the dielectric waveguide was one third of the required length.

3.2 *ATTENUATION MEASUREMENTS OF THE MICROWAVE SYSTEM*

In order to evaluate the attenuation in the microwave transmission system an experimental arrangement shown in Fig. 3.1 was used. The tracking system was operating in the seeking mode. An oscilloscope operating in the $x - y$ mode was connected to the output of the system. A section of an X-band rectangular waveguide was then substituted for the microwave line to obtain the reference (full reflection) level. Since the detector operated in the square law region the attenuation could be measured directly. The output level of the detector was also measured while the system was tracking.

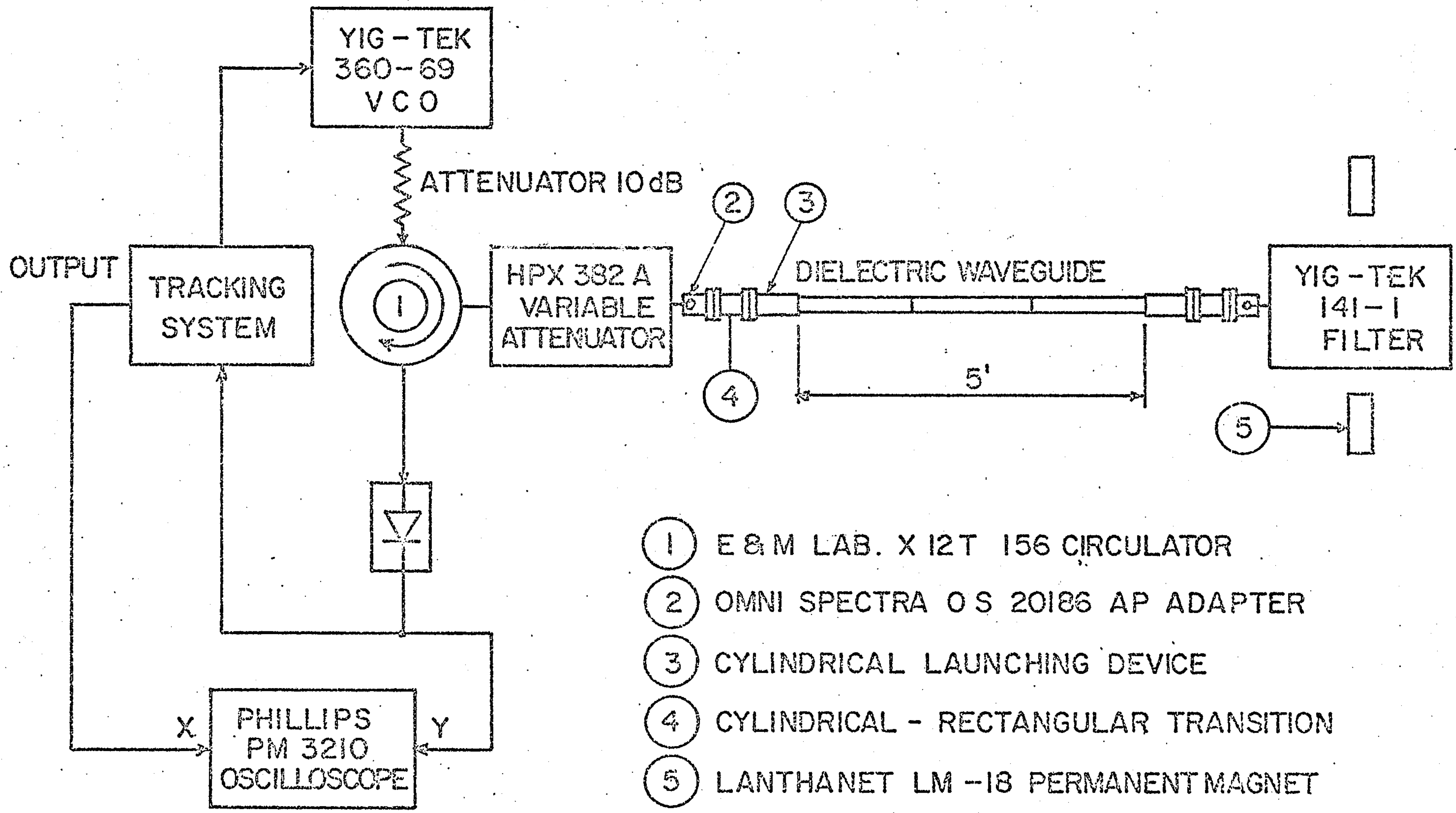

Figure 3.1 : TEST SETUP FOR MEASURING MICROWAVE SYSTEM ATTENUATION

3.3 *EXPERIMENTAL ARRANGEMENT FOR DYNAMIC MEASUREMENTS*

An experimental setup for dynamic measurements is shown in Fig. 3.2. The YIG filter was coupled to the locking system by means of an *X*-band attenuator in order to simulate the attenuation in the microwave system. The open loop gain was made adjustable. The incoming and outgoing signals were separated by a circulator. Two tuning coils were placed near the YIG filter and driven from a function generator to provide variations in the YIG filter resonant frequency. The coils were 50 mm (2 in.) in inner diameter, 12 mm (1/2 in.) in length and consisted of 500 turns of a 0.5 mm diameter wire.

The YIG filter used was a custom made YIG-TEK model 141-1. It was mounted in a Plexiglas holder with two adjustable permanent magnets which were used to set the operating point of the filter.

3.4 *MEASUREMENT OF FREQUENCY AND PHASE RESPONSES*

A test setup for frequency and phase response measurements is shown in Fig. 3.2. A 0-40 kHz function generator was used to supply the tuning coils. The coils were positioned near the YIG filter so that their magnetic field could tune the filter. The coil current was measured using a resistor in series with the tuning coils.

For convenience the frequency response was obtained indirectly. Both the coil input current vs. frequency characteristic (Fig. 3.3) and the output voltage vs. frequency characteristic were plotted, and the frequency response then was calculated.

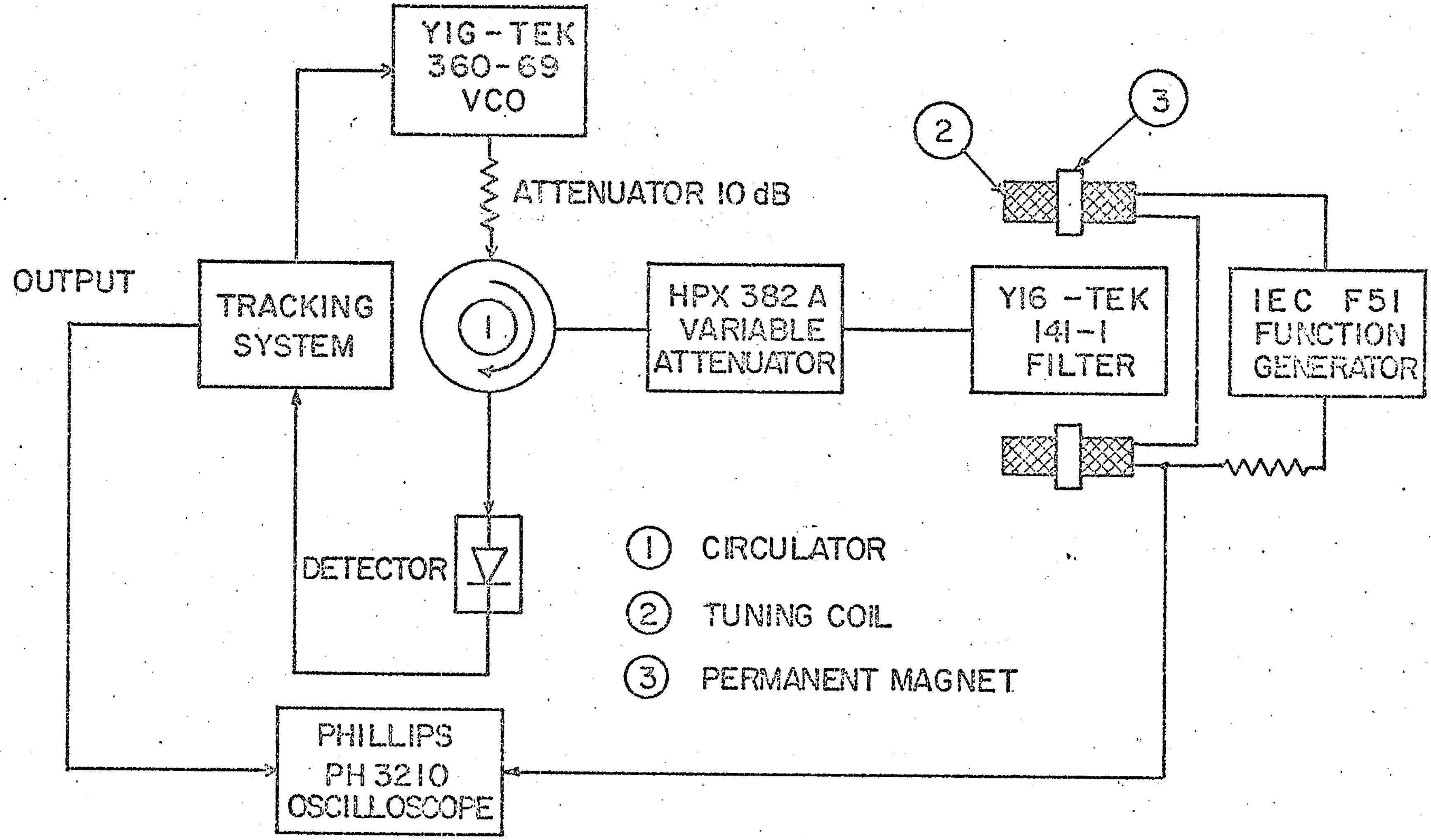

Figure 3.2 : TEST SETUP FOR DYNAMIC RESPONSE MEASUREMENTS

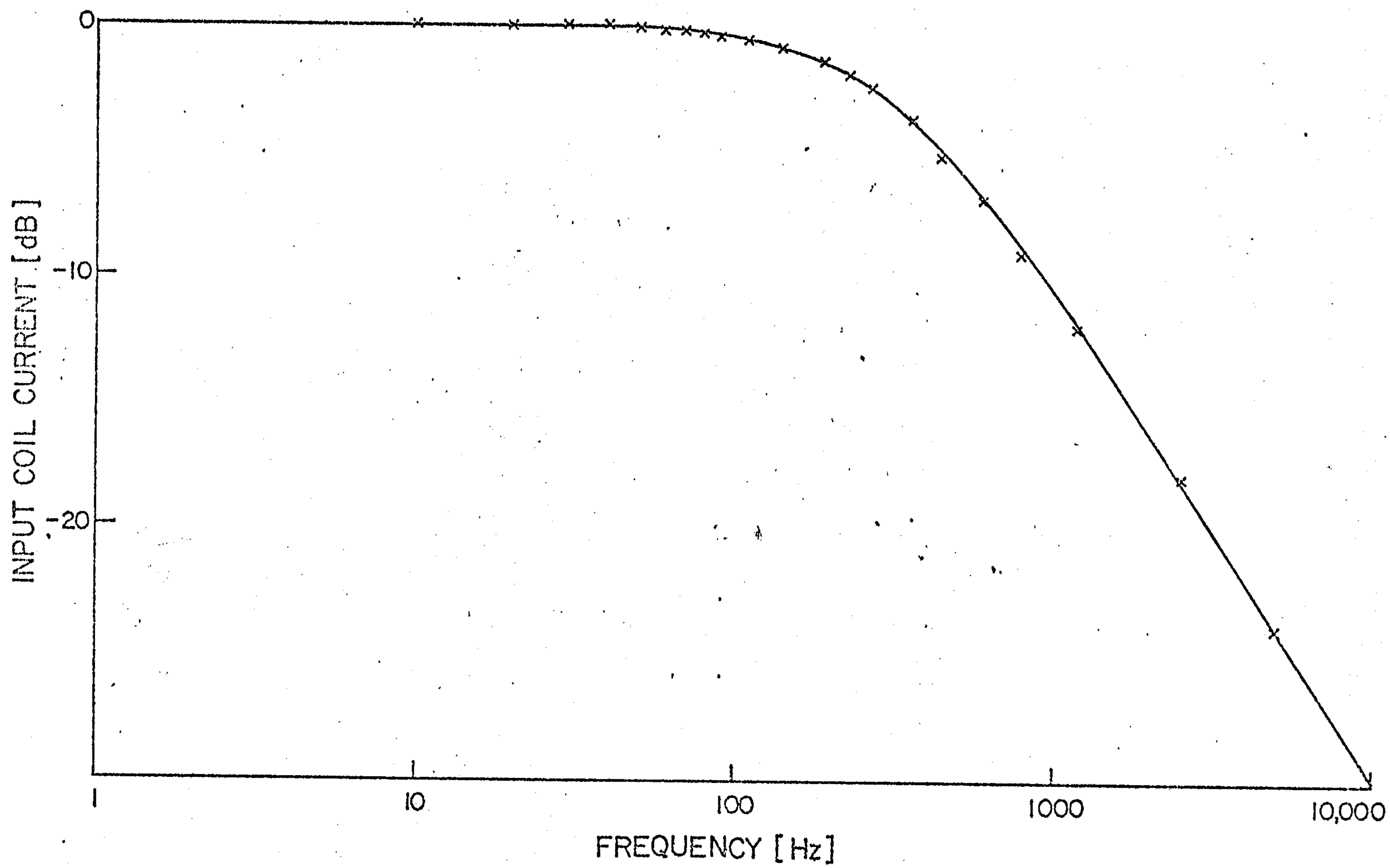

Figure 3.3 : INPUT COIL CURRENT FREQUENCY RESPONSE

The phase response was obtained directly. Care had to be taken during these measurements to avoid large input signals which could cuase non-linear operation of the system.

3.5 *MEASUREMENT OF THE RISE TIME*

A test setup for rise time measurement is shown in Fig. 3.2. A square wave function generator was used to feed the tuning coils. A resistor in series with the tuning coils was selected to obtain a current square wave with a rise time fast compared with that of the tracking system. The rise time was defined as the time between 10% and 90% of the final value.

3.6 *SLEW RATE*

A test setup shown in Fig. 3.2 was used to measure the slew rate of the system at different frequencies. The slew rate is defined as a maximum rate of the output signal at which the system can track expressed in *V/s*. A sine-wave function generator was used to feed the tuning coils. The current amplitude was increased until the system became unlocked (started seeking). The maximum output amplitude before the system started seeking was measured in a frequency range from 0.1 to 10 kHz. The slew rate was calculated at different frequencies.

3.7 HARMONIC DISTORTION

The harmonic distortion was evaluated using a test setup shown in Fig. 3.2. A sine-wave function generator was used to supply the tuning coils. A spectrum analyser was connected to the output of the tracking system. The input signal amplitude was kept small enough to avoid non-linear operation. The spectrum of the input current signal was compared with that of the output.

3.8 OUTPUT SIGNAL VERSUS SUPPLY VOLTAGE

The measurements were done using a test setup shown in Fig. 3.4. A variac was used to change the supply voltage. The VCO was locked to the resonant frequency of the YIG filter which was adjusted by means of the magnets until the output of the system reached a level of 5 V. The power supply voltage was then varied over a range from 75 to 135 V.

3.9 NOISE

A test setup shown in Fig. 3.5 was used for noise measurements. The VCO was locked to the resonant frequency of the YIG filter resulting in a D.C. signal at the output of the system. An oscilloscope was connected to the output and the noise voltage level was measured. A variable attenuator was used to change the open loop gain.

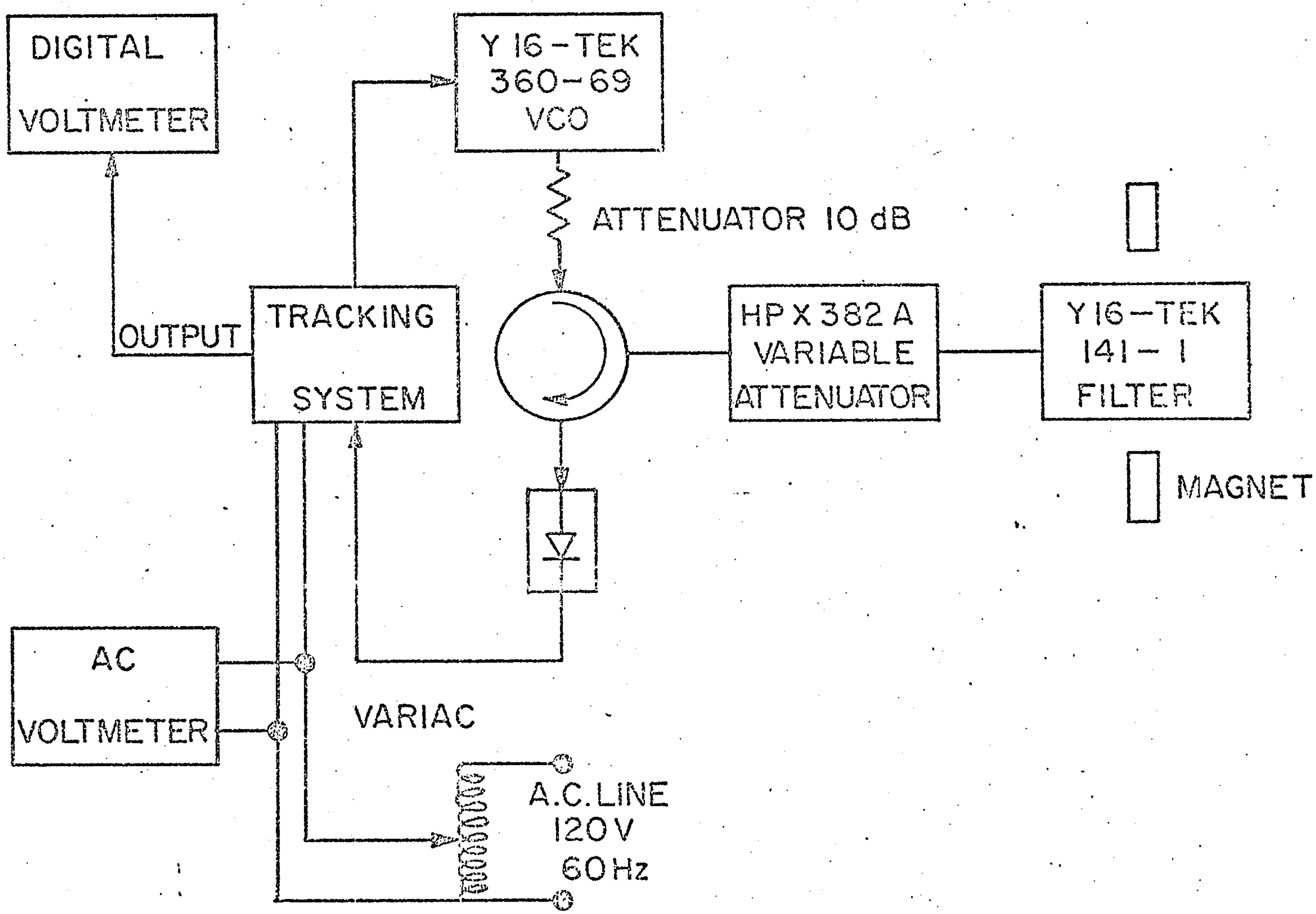

Figure 3.4 : TEST SETUP FOR MEASURING SUPPLY VOLTAGE EFFECTS

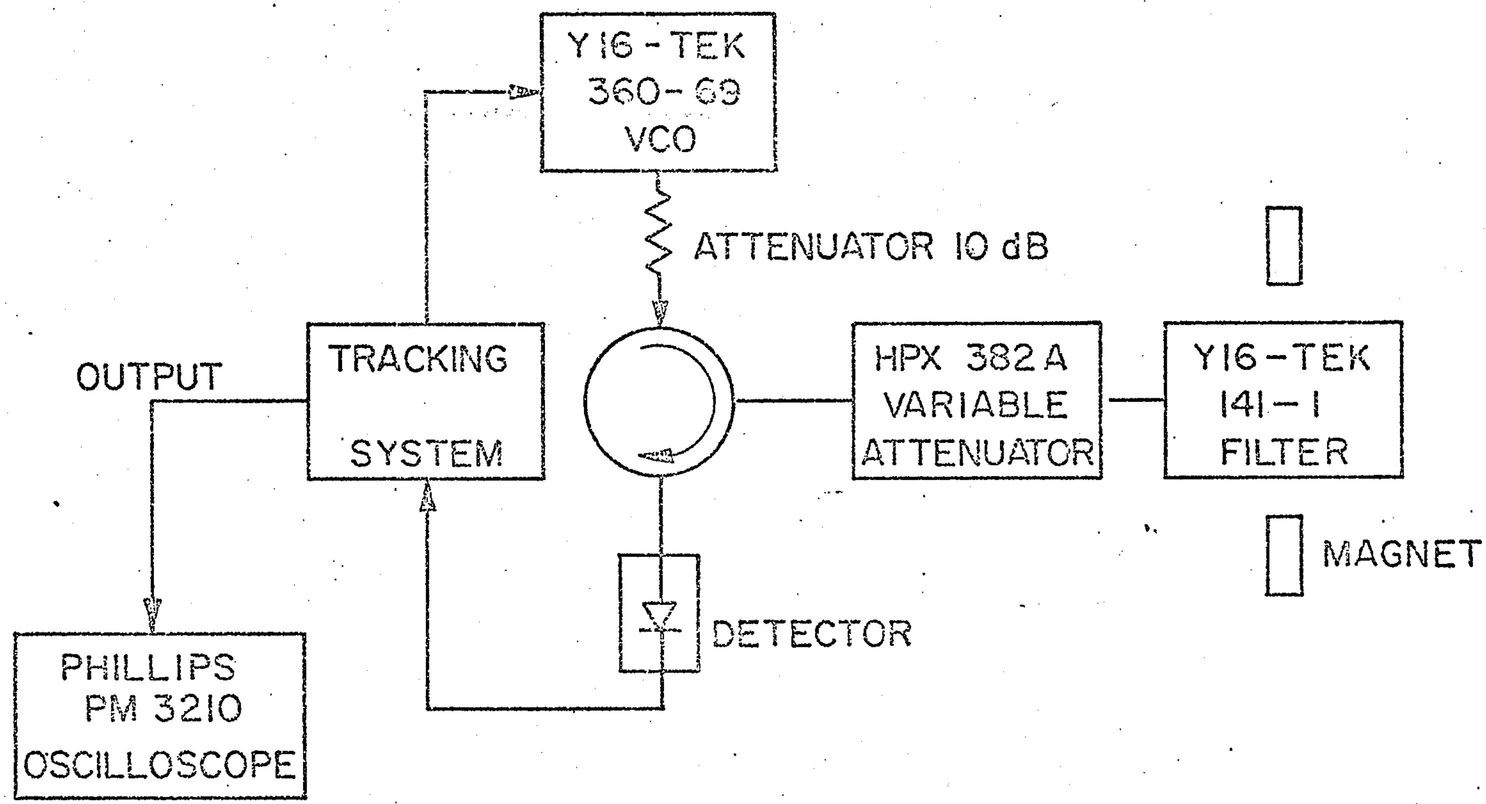

Figure 3.5 : TEST SETUP FOR MEASURING THE OUTPUT NOISE LEVEL

3.10 A.C. OUTPUT TEMPERATURE BEHAVIOUR

A test setup shown in Fig. 3.6 was used to observe the behaviour of the tracking system in a temperature range from -35°C to +60°C. The amplitude of the coil current was increased until the maximum slew rate of the system was obtained at the output. An oscilloscope connected to the output was used to determine whether the system was tracking.

3.11 D.C. OUTPUT TEMPERATURE BEHAVIOUR

A test setup shown in Fig. 3.7 was used to observe the output signal of the tracking system over a range of temperatures from 20°C to 60°C. The VCO was locked to the resonant frequency of a tunable cavity placed outside the environmental chamber. A tunable cavity was chosen to make sure that the input signal would not vary with the ambient temperature.

The variations of the output were observed using a voltmeter. A frequency meter was also used to observe frequency variations of the VCO.

3.12 TEMPERATURE BEHAVIOUR OF THE BIASING MAGNETIC CIRCUIT

A test setup shown in Fig. 3.8 was used. The YIG filter mounted in the holder was placed into the climatic chamber. The VCO was locked to the resonant frequency of the YIG filter. An arbitrary operating point was selected by adjusting the separation of the permanent magnets. A voltmeter connected to the output of the tracking system determined the output signal.

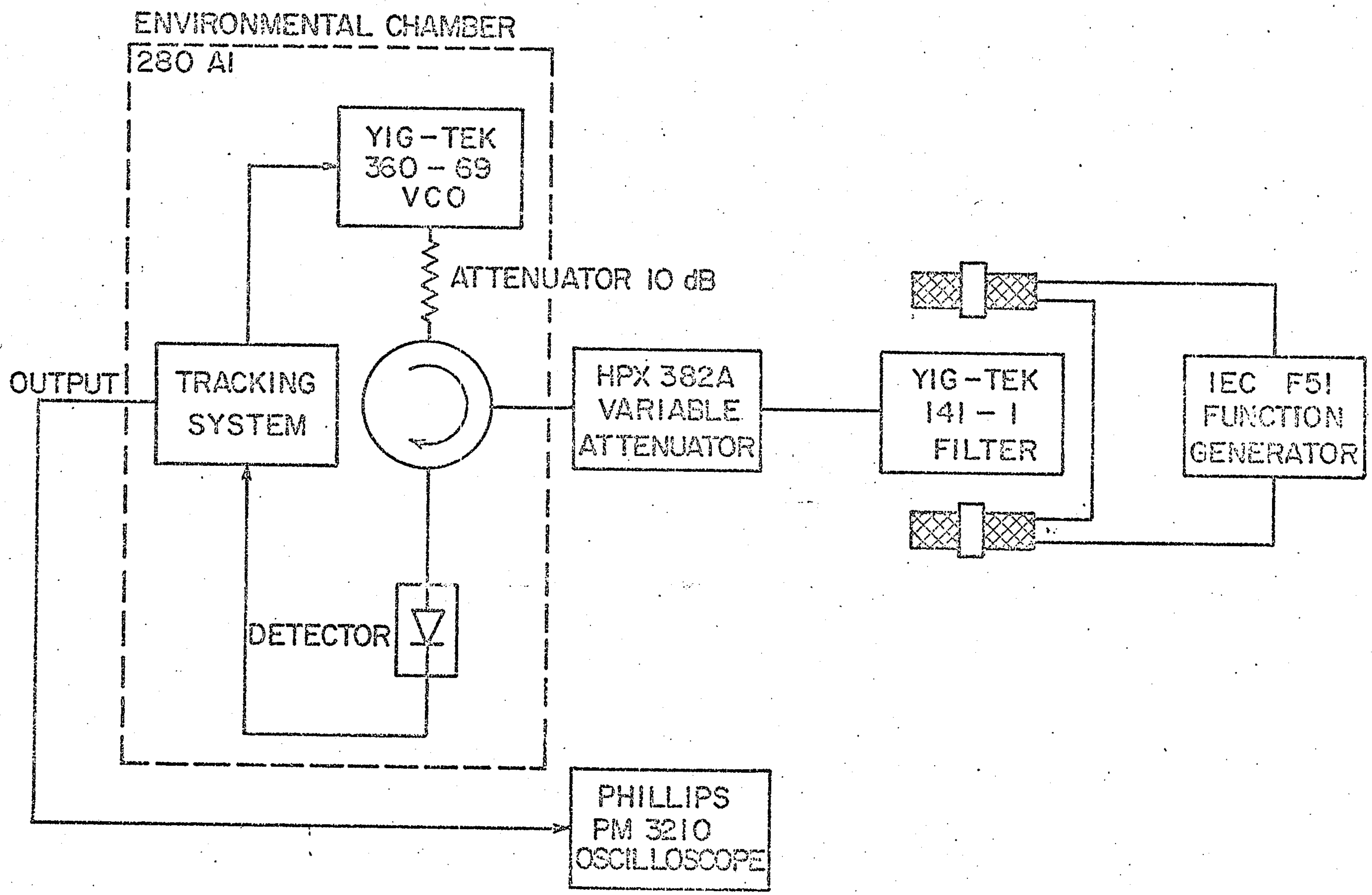

Figure 3.6 : ARRANGEMENT FOR A.C. OUTPUT TEMPERATURE BEHAVIOUR TEST

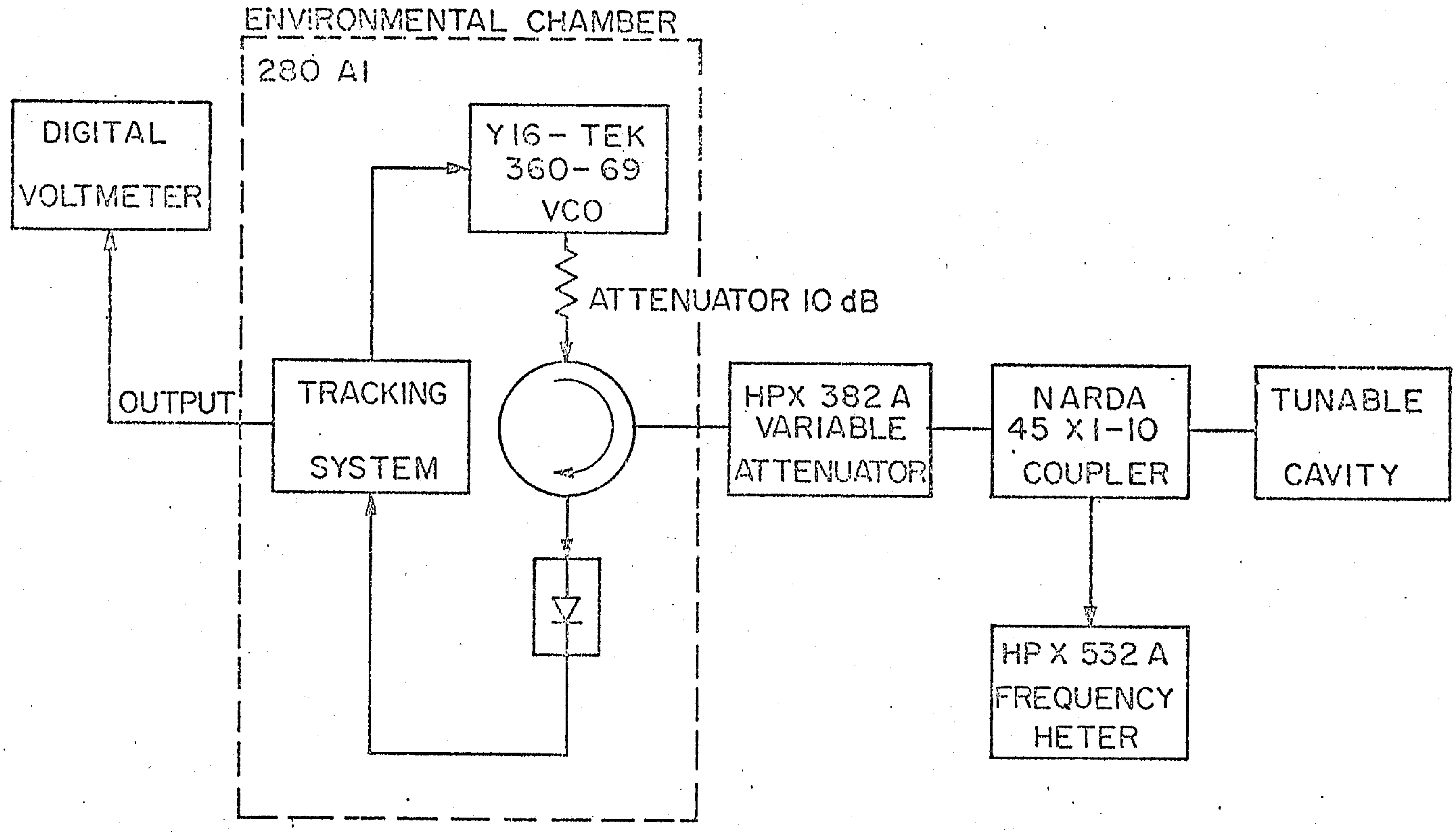

Figure 3.7 : ARRANGEMENT FOR D.C. OUTPUT TEMPERATURE BEHAVIOUR TEST

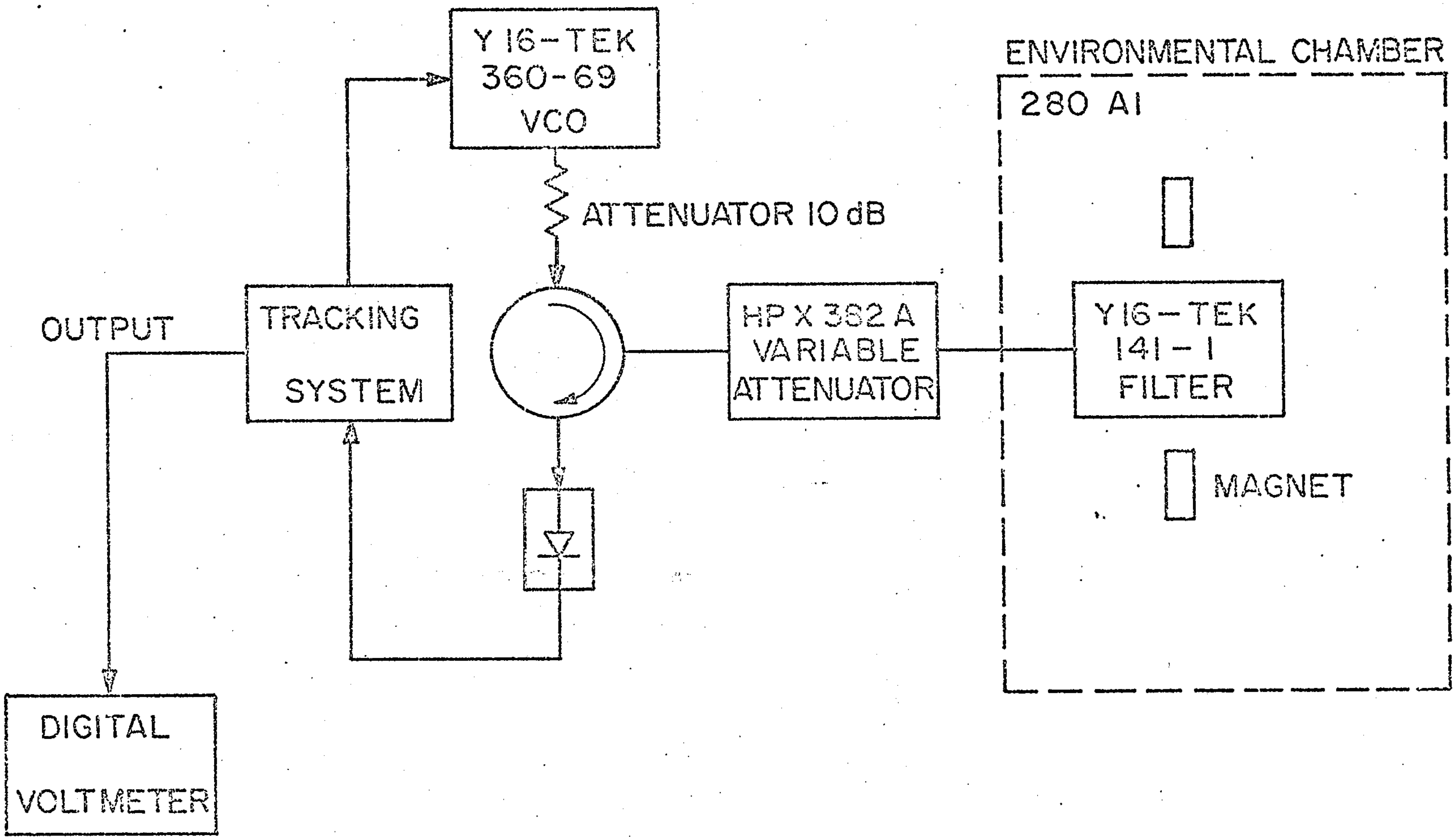

Figure 3.8 : ARRANGEMENT FOR BIASING MAGNETIC CIRCUIT TEMPERATURE TEST

3.13 *CALIBRATION OF THE SYSTEM*

The output voltage vs. resonant frequency of the YIG filter was measured using an experimental setup shown in Fig. 3.9. The VCO was locked to the YIG's resonant frequency. The coil current was varied in order to change the magnetic field strength and thereby the resonant frequency of the filter.

Two other arrangements unvolving high current generators were used. The first one with a high A.C. current source, shown in Fig. 3.10 and 3.11, was used in the laboratory to eliminate the temperature influence on the biaising magnetic circuit. The second one, assembled in the Manitoba Hydro Dorsey converter station, utilized a high D.C. current source. The measurement setup is shown in Fig. 3.12 and 3.13. In both cases, output voltage of the tracking system vs. the amplitude of the current in the bus line were measured.

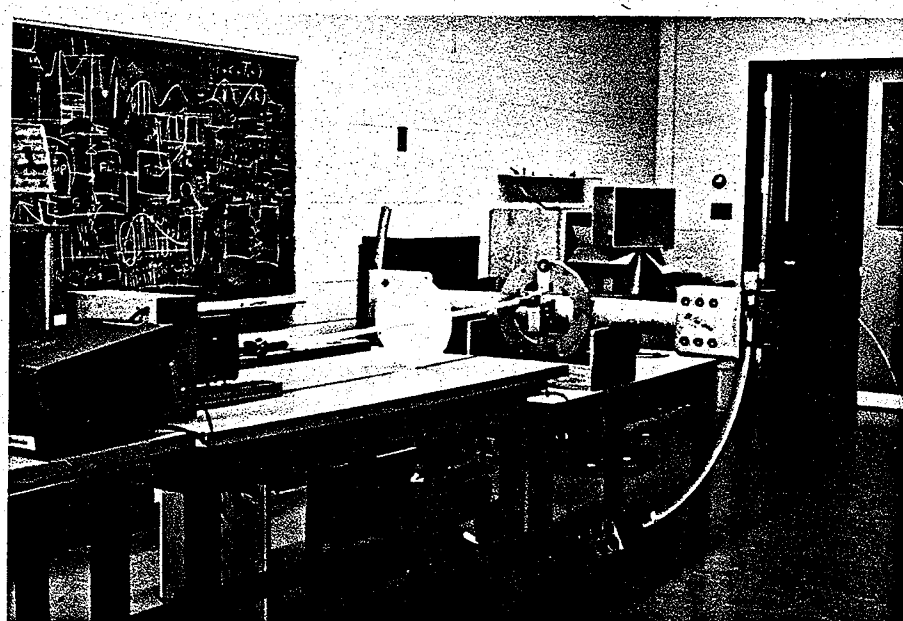

Figure 3.11 : EXPERIMENTAL ARRANGEMENT FOR A.C. CALIBRATION

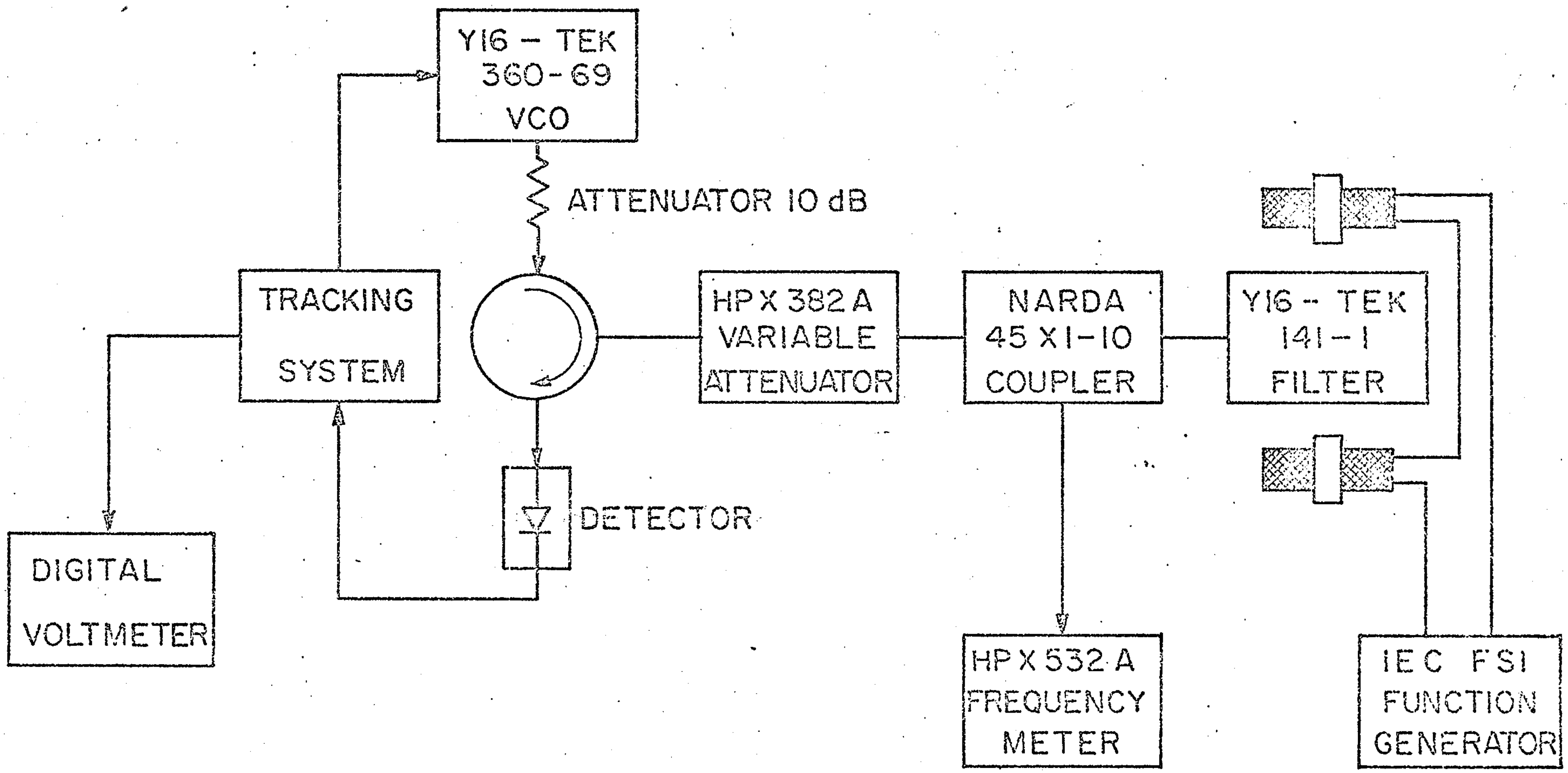

Figure 3.9 : TEST SETUP FOR CALIBRATING THE SYSTEM

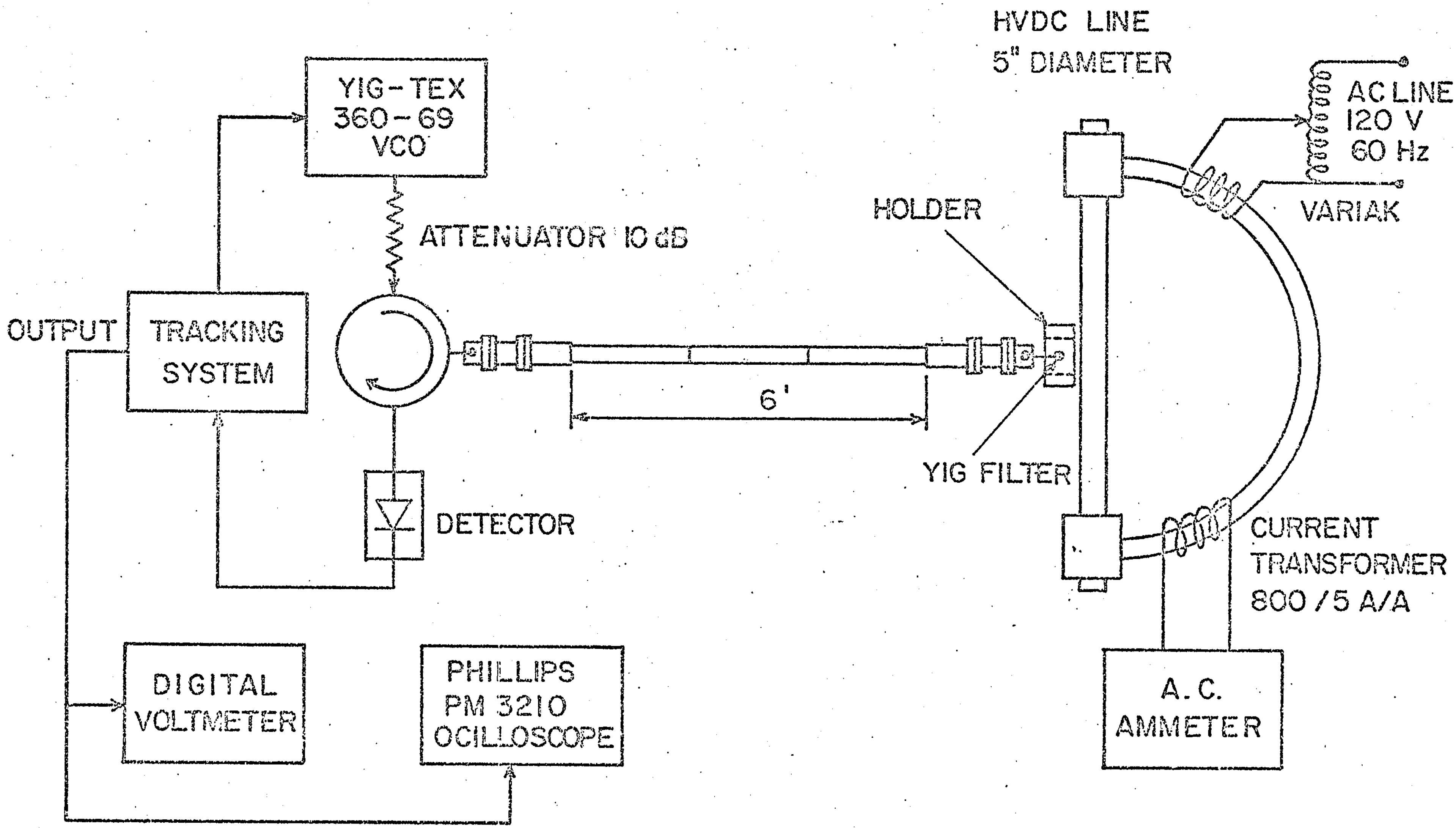

Figure 3.10 : TEST CIRCUIT FOR A.C. CALIBRATION

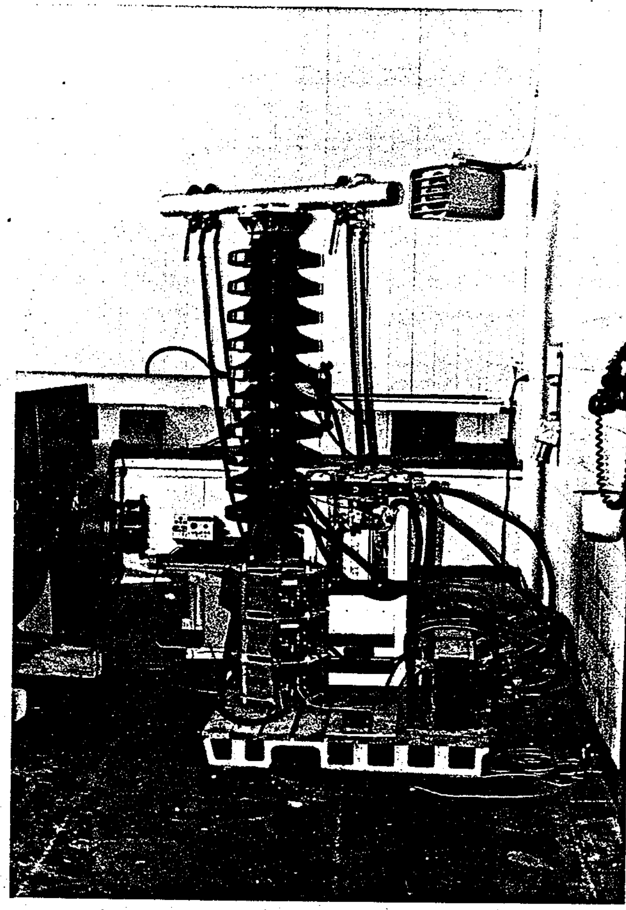

Figure 3.12 : EXPERIMENTAL ARRANGEMENT FOR D.C. CALIBRATION

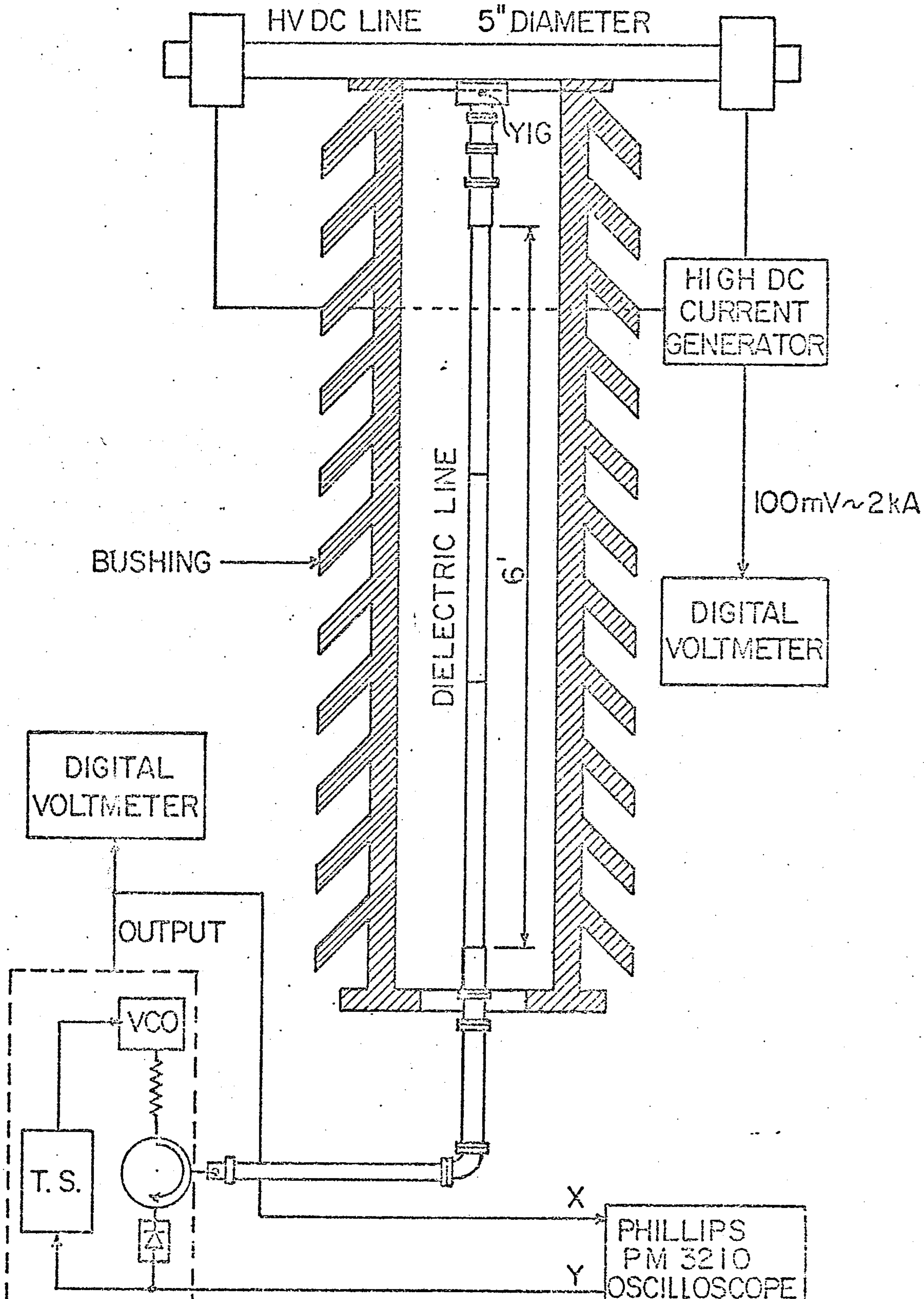

Figure 3.13 : TEST SETUP FOR HIGH D.C. CURRENT CALIBRATION

Chapter 4

EXPERIMENTAL RESULTS

4.1 *ATTENUATION OF THE MICROWAVE SYSTEM*

Return loss measurements were carried out in a frequency range from 10 to 11 GHz. Theoretical calculations indicated that a frequency band of 400 MHz was required to cover the whole range of test currents. A frequency range where attenuation was minimal was selected for the prototype.

Figure 4.1 illustrates the return loss vs. frequency over a frequency range from 10.4 to 10.8 GHz. The system is matched at the resonant frequency of the filter. By comparison with the full reflection level (Fig. 4.3), a return loss varying between 2.5 and 5 dB was calculated.

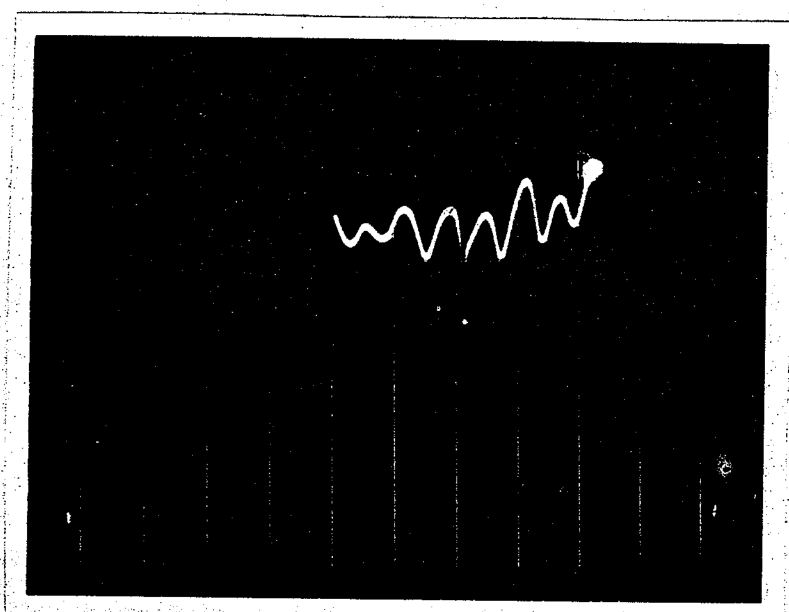

Figure 4.1 : RETURN LOSS VS. FREQUENCY
y - axis : output detector. 0.1 V/div.
x - axis : VCO frequency. 100 MHz/div.

The output detector level when the system is tracking is shown in Fig. 4.2.

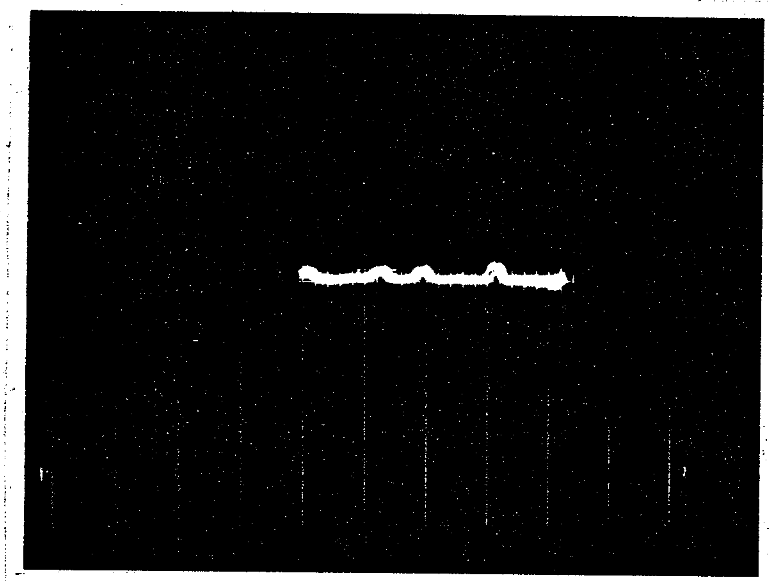

Figure 4.2 : DETECTOR OUTPUT VS. FREQUENCY; TRACKING SYSTEM ON.
y - axis : detector output. 0.1 V/div.
x - axis : VCO frequency. 100 MHz/div.

It was found that in the selected frequency range the YIG filter is quite well matched at resonance. These measurements were done with a dielectric waveguide of one third of the required length. However, it is known [8] that the losses in the dielectric waveguide (about 0.15 dB/m) remain small compared with the losses in the launching devices.

It was verified experimentally that most of the power is transmitted inside the dielectric, the electromagnetic field does not expand outside the rod [8] and therefore would not be perturbed by a bushing insulator surrounding the waveguide.

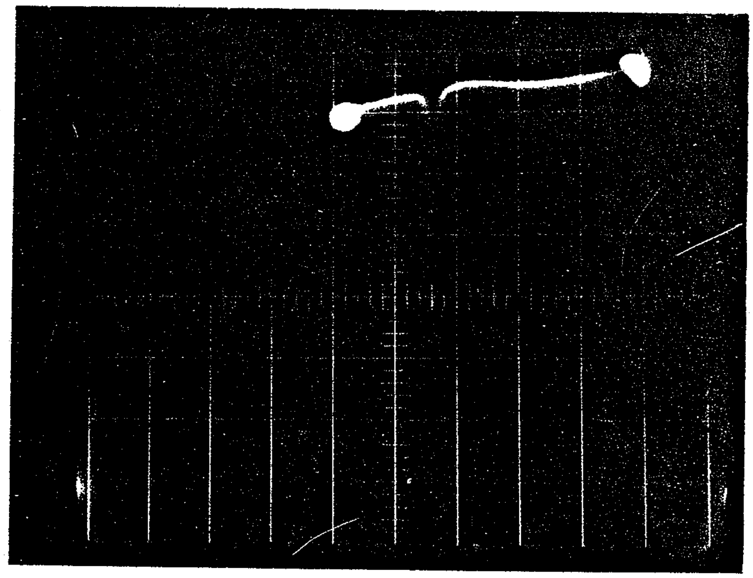

Figure 4.3 : FULL REFLECTION LEVEL VS. FREQUENCY
y - axis : detector output. 0.1 V/div.
x - axis : VCO frequency. 100 MHz/div.

4.2 *FREQUENCY AND PHASE RESPONSES*

Frequency and phase responses of the system for two different attenuations in the microwave line are shown in Fig. 4.4. The value of 6dB return loss was chosen as a maximum attenuation expected in the microwave system. Small differences appear only at higher frequencies (above 10 kHz in the amplitude characteristic and above 1 kHz for the phase).

4.3 *TRANSIENT RESPONSE*

The rise time of the system was measured for different attenuations in the microwave system. The rise time of the input square wave was 5μs.

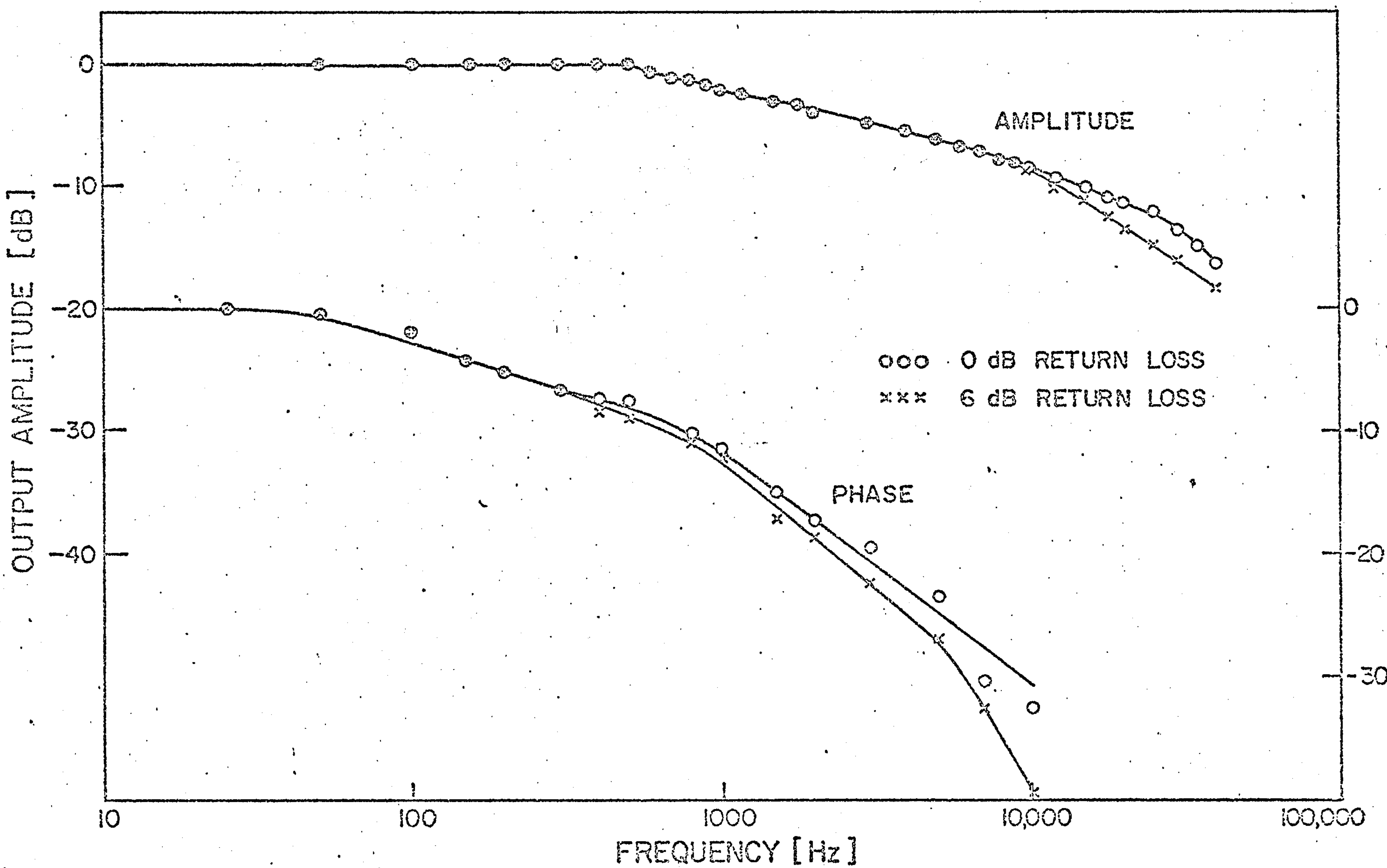

Figure 4.4 : SYSTEM FREQUENCY RESPONSES

For a return loss of 6 dB the rise time of the system was 300 μs.

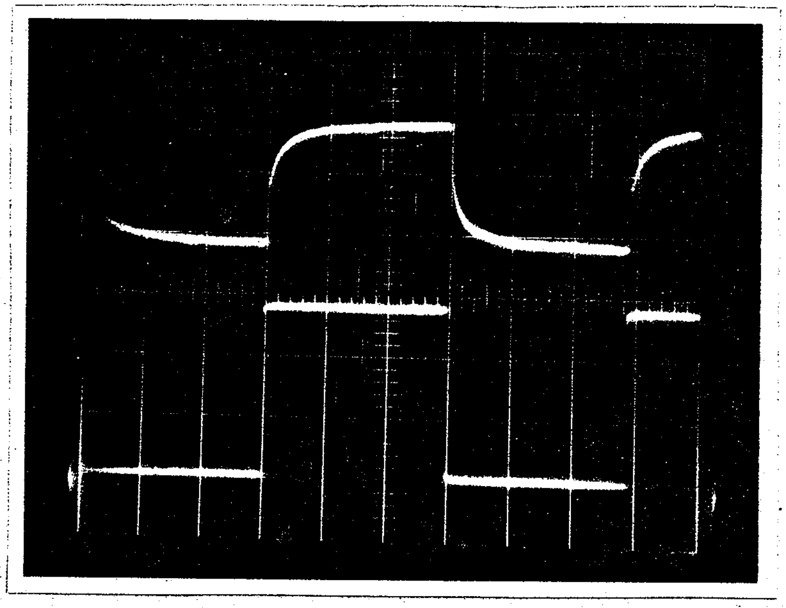

Figure 4.5 : TRANSIENT RESPONSE OF THE SYSTEM

bottom : input signal 10 V/div. or 1.5 mA/div.
top : output signal 100 mV/div.
time scale : 1 ms/div.

4.4 SLEW RATE

The slew rate of the system is plotted in Fig. 4.6 as a function of frequency. As expected, it changes very little with frequency since it depends only on the characteristic of the YIG filter and the open loop gain. The average value was found to be about 4 V/ms which is equivalent to 12 kA/ms in the bus (see the calibration curve of the system: Fig. 4.17). No significant changes of the characteristic were observed for the return

Figure 4.6 : SLEW RATE CHARACTERISTIC

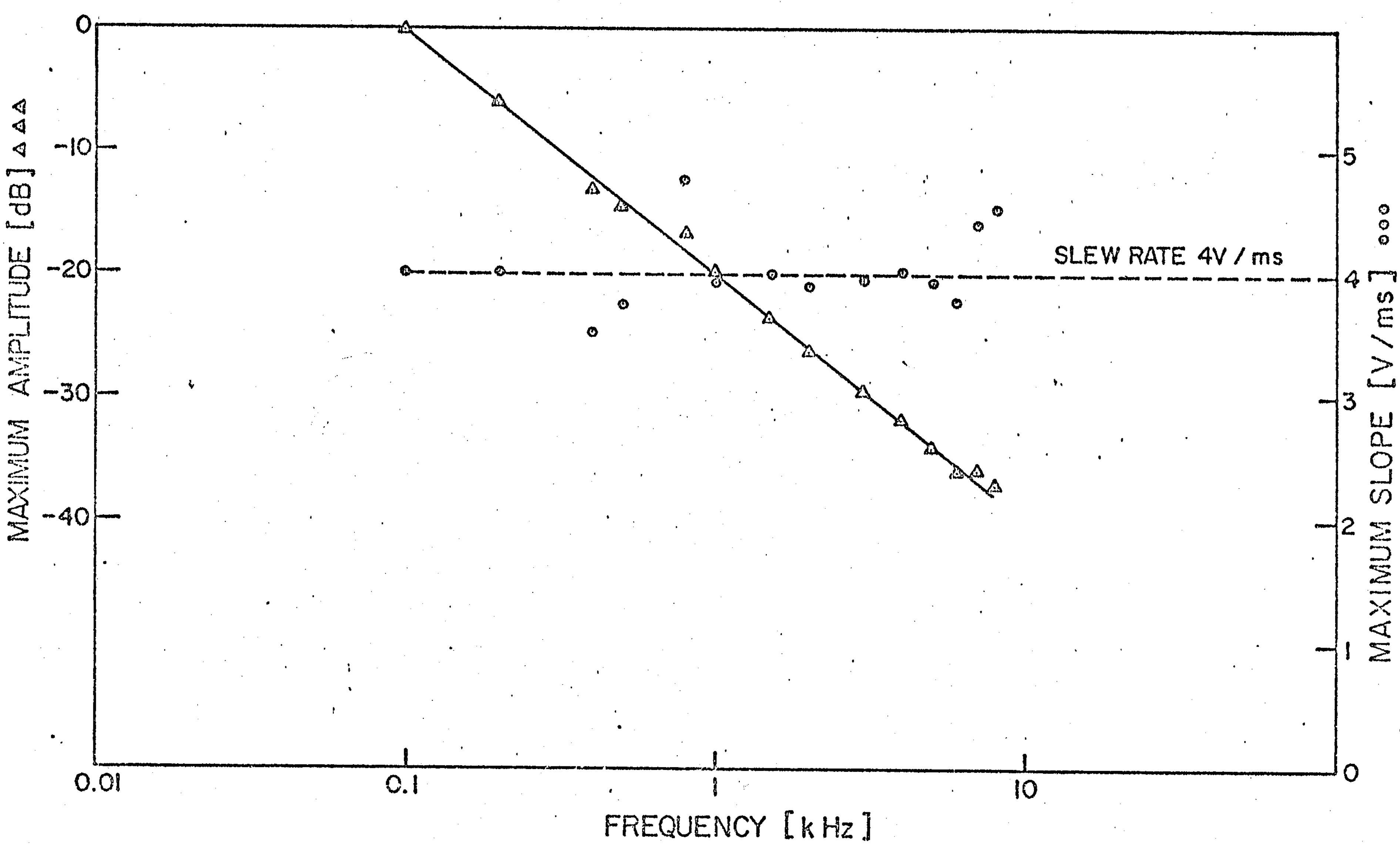

losses up to 10dB. Above 10dB level, the system becomes nonlinear.

4.5 *HARMONIC DISTORTIONS*

The harmonic distortions measurements were done at input signal frequencies of 100 Hz and 1000 Hz. The output signal amplitude was 1 V. peak-to-peak. The harmonic distortions were computed as the ratio of the square root of the sum of the squared amplitudes of the harmonics to the amplitude of the fundamental.

At both frequencies the harmonic distortions of the input signal were below 0.07% (Fig. 4.7). The harmonic distortions of the output signal were 0.08% at 100 Hz and 0.18% at 1000 Hz (Fig. 4.8 and 4.9). These results indicate the high linearity of the system.

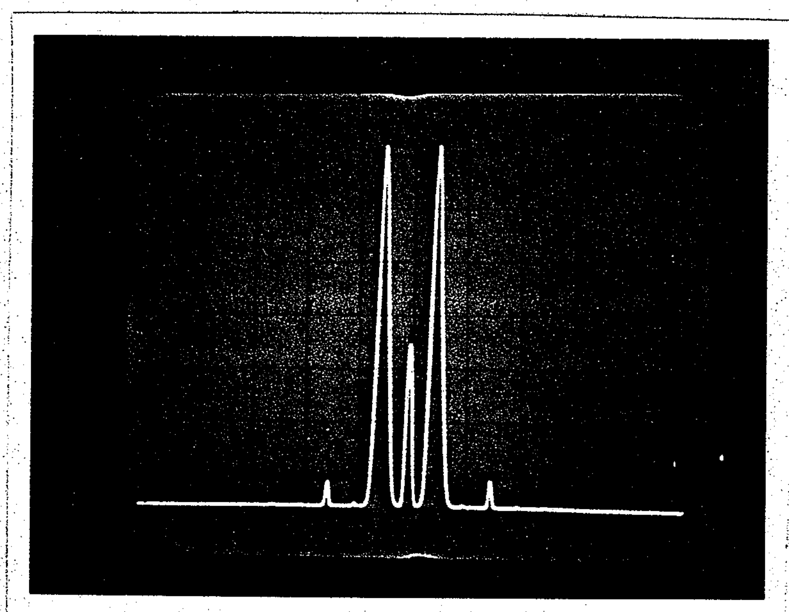

Figure 4.7 : INPUT FREQUENCY SPECTRUM
y - axis : 10 dB/div.
x - axis : 200 Hz/div.

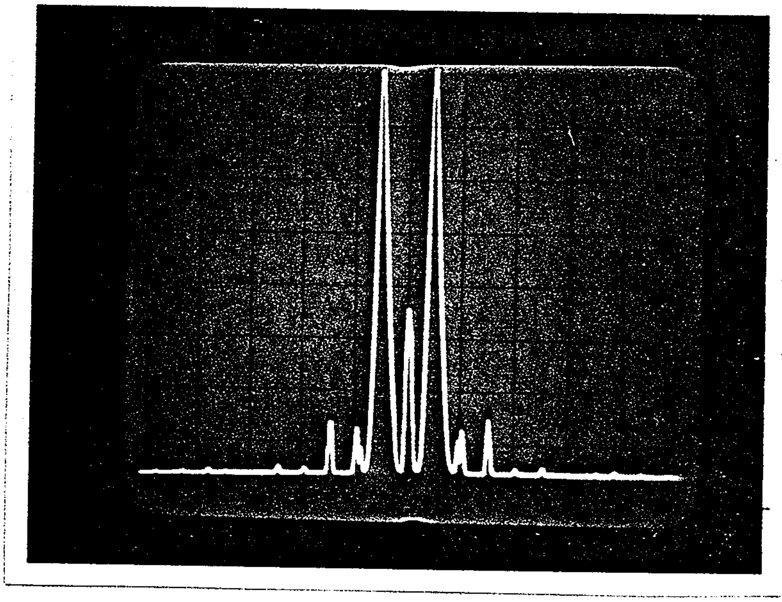

Figure 4.8 : OUTPUT FREQUENCY SPECTRUM (100 Hz)
y - axis : 10 dB/div.
x - axis : 200 Hz/div.

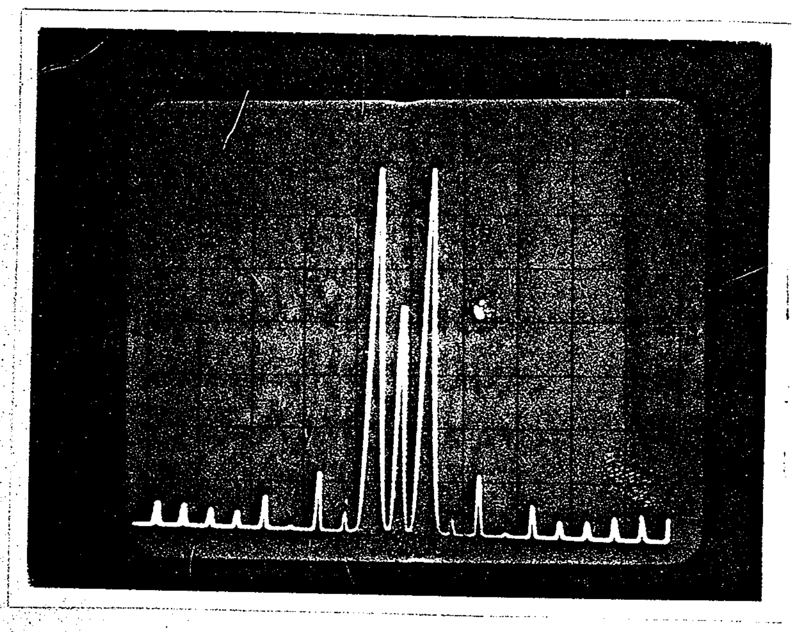

Figure 4.9 : OUTPUT FREQUENCY SPECTRUM (1000 Hz)
y - axis : 10 dB/div.
x - axis : 2 kHz/div.

4.6 OUTPUT SIGNAL VS. SUPPLY VOLTAGE

No significant variations of the output signal level were observed when the supply voltage was varied from 75 to 135 V. Below 70 V. the system fails to operate.

4.7 NOISE MEASUREMENT

The noise level for 6 dB return loss was found to be 2 mV. The noise level should depend on the open loop gain, however, no changes were observed when the open loop gain was increased by 6 dB. A 60 Hz component of 2 mV (peak-to-peak) was observed (Fig. 4.10). The resulting signal-to-noise ratio for a nominal line current of 2 kA is 50 dB abd is 25 dB for 100 A line current.

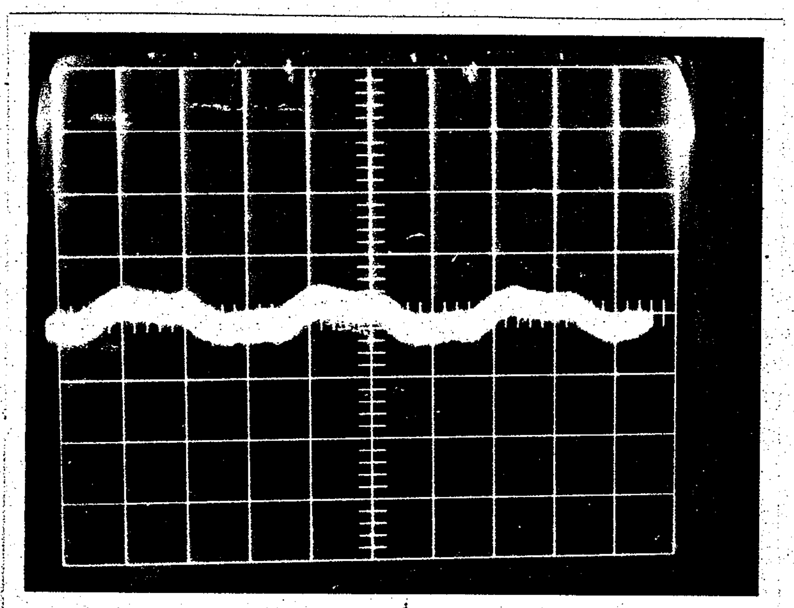

Figure 4.10 : D.C. OUTPUT SIGNAL AT THE NOISE LEVEL
y - axis : 5 mV/div.
x - axis : 5 ms/div.

4.8 A.C. OUTPUT TEMPERATURE BEHAVIOUR

With 3dB return loss, the system was tracking at its maximum slew rate over a temperature range from -15°C to +60°C. Below -15°C the open loop gain became too low to keep the system tracking. The reason for this is that the open loop gain decreased with the temperature. By decreasing the return loss to zero, the system was kept tracking down to -35°C.

4.9 D.C. OUTPUT TEMPERATURE BEHAVIOUR

The D.C. output voltage offset vs. temperature characteristic is shown in Fig. 4.11. The VCO frequency did not vary more than 0.03 MHz during the test. However, a temperature dependence on the output was detected. This effect is attributed to the temperature sensitivity of the YIG tuned oscillator.

4.10 TEMPERATURE STABILITY OF THE BIASING MAGNETIC CIRCUIT

Figure 4.12 depicts the output voltage and the frequency change of the VCO as a function of temperature. A strong temperature dependence is evident. In a range of temperature from +20°C to +50°C, the output signal varied over almost the entire available range. The effect is most probably due to the thermal expansion of the magnets' holder.

For the selected operating point of the magnetic circuit the magnetic field strength in the gap strongly depends on the distance between the magnets (Fig. 2.6).

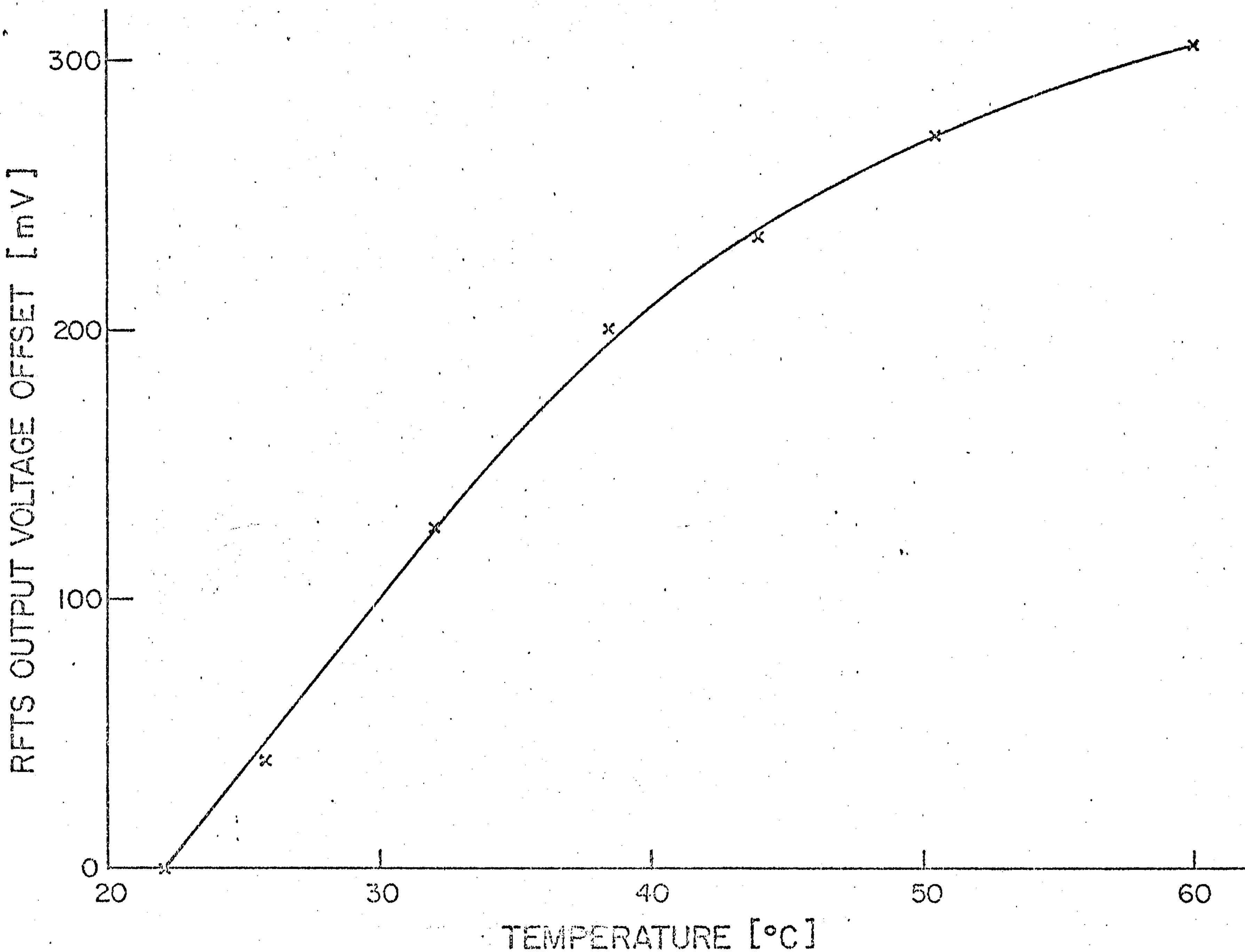

Figure 4.11 : TEMPERATURE EFFECT ON THE TRACKING SYSTEM OUTPUT

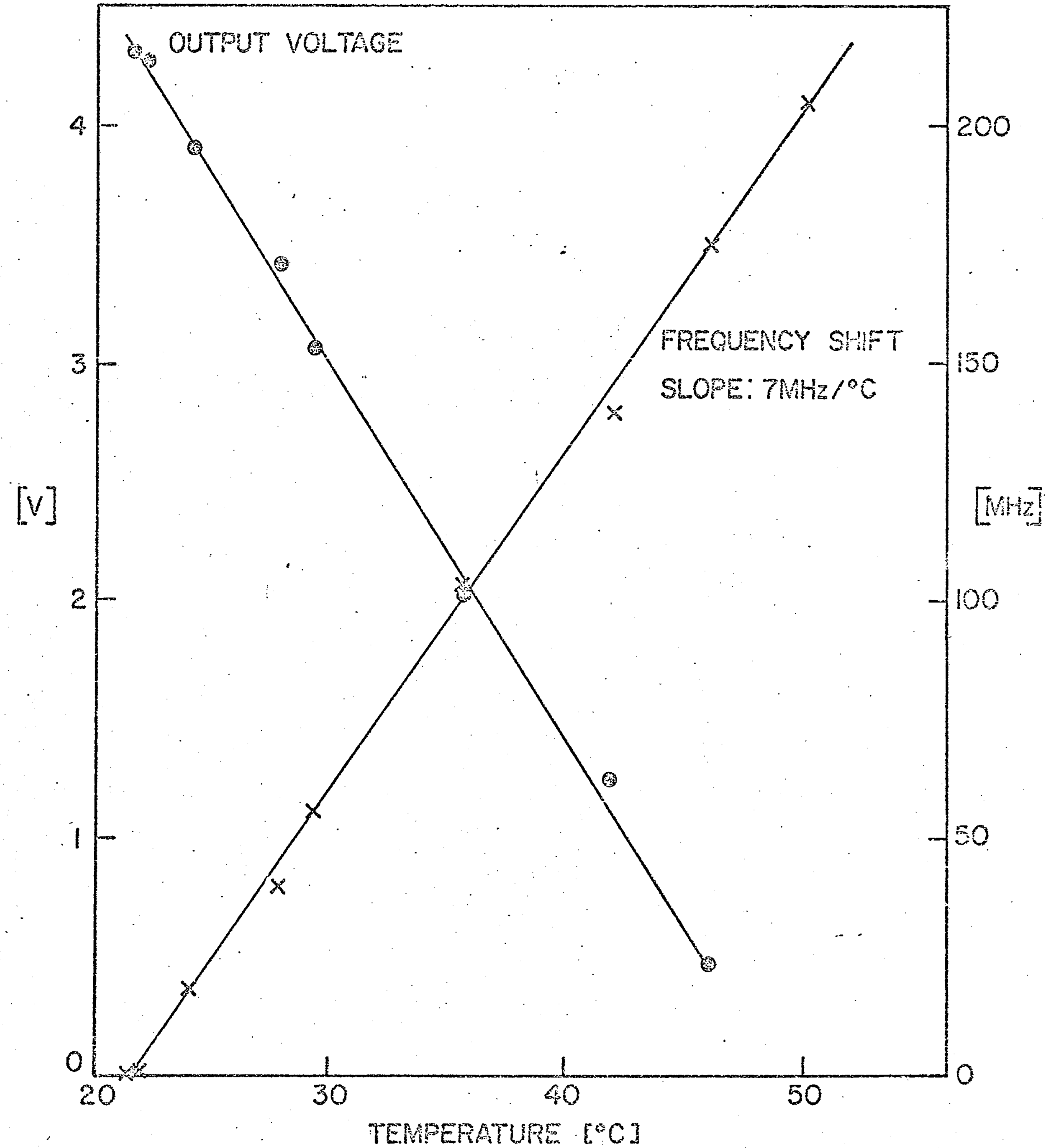

Figure 4.12 : TEMPERATURE EFFECT ON THE BIASING MAGNETIC CIRCUIT

4.11 *CALIBRATION OF THE SYSTEM*

The input-output transfer characteristic of the current transducer is shown in Fig. 4.13. The straight line equation was obtained using the least square mean method. The correlation coefficient 0.997 indicates very high linearity of the system. No hysteresis effects were observed.

The results of the A.C. current calibration are plotted in Fig. 4.14. Two different flanges (shown in Fig. 4.15 and 4.16) were used. In the arrangement shown in Fig. 4.15, the YIG sphere was positioned 18 mm from the outside surface of the conductor.

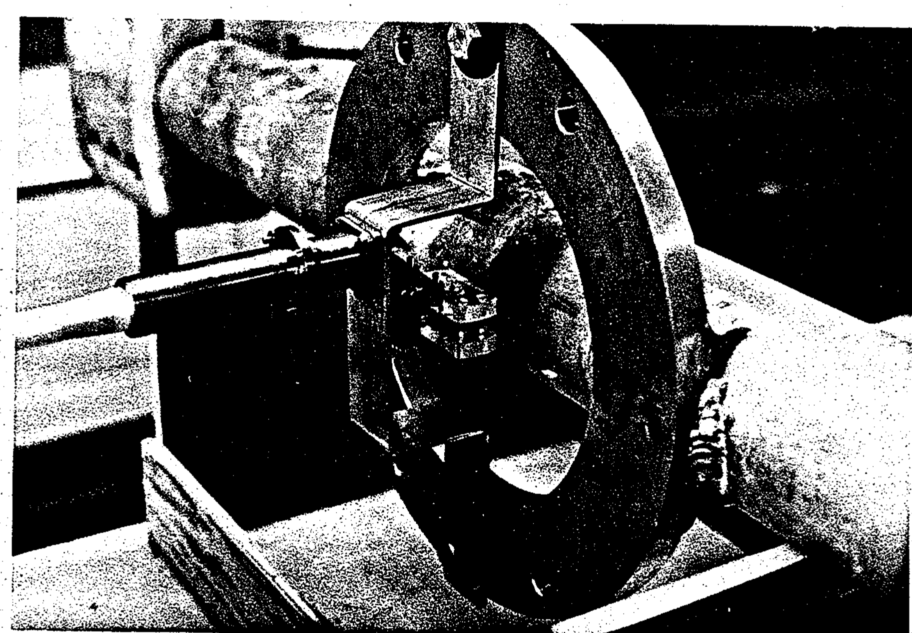

Figure 4.15 : HOLLOW FLANGE

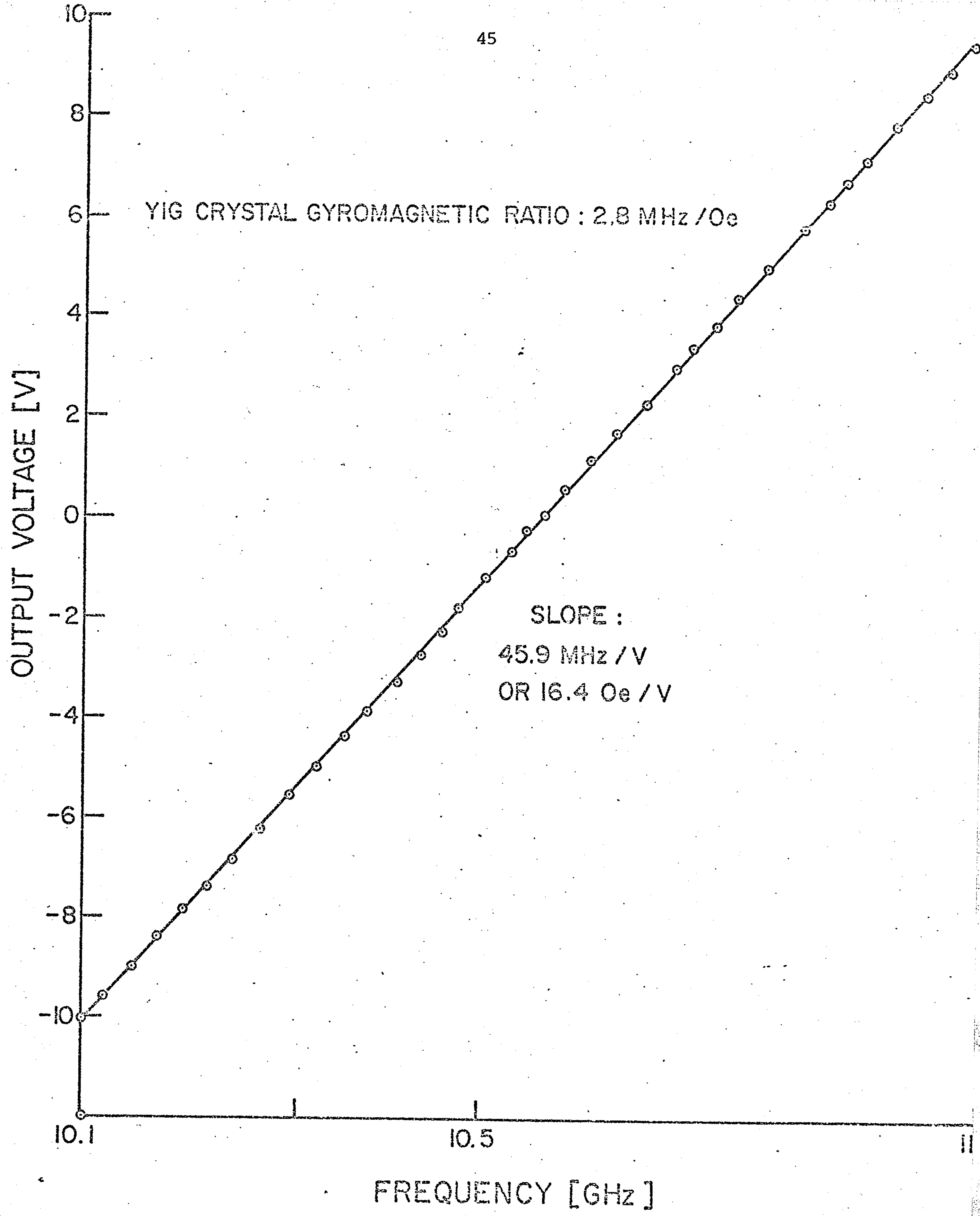

Figure 4.13 : TRACKING SYSTEM CALIBRATION

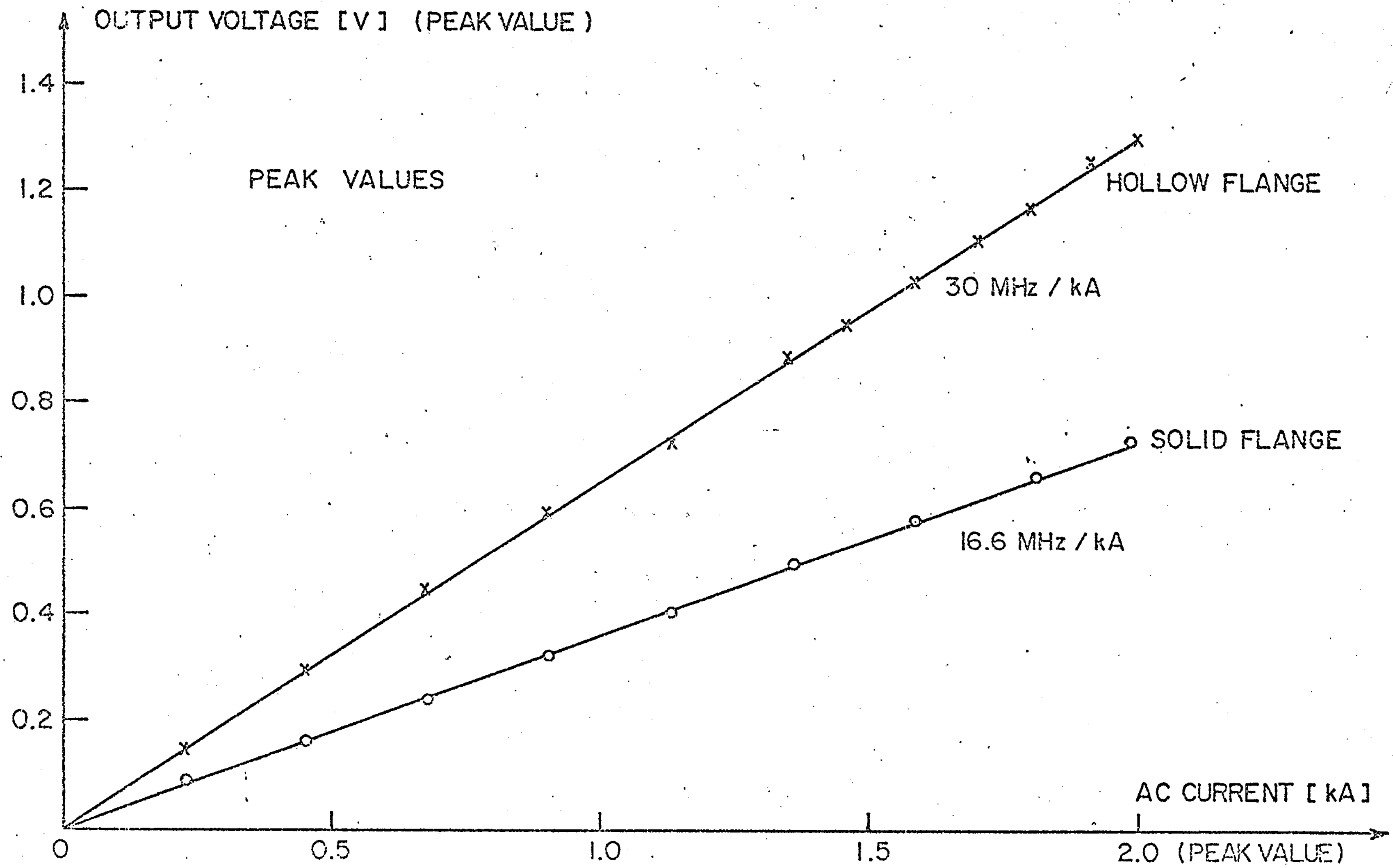

Figure 4.14 : A.C. CURRENT CALIBRATION

In the second case shown in Fig. 4.16, it was placed 12.5 mm from the surface of the conductor.

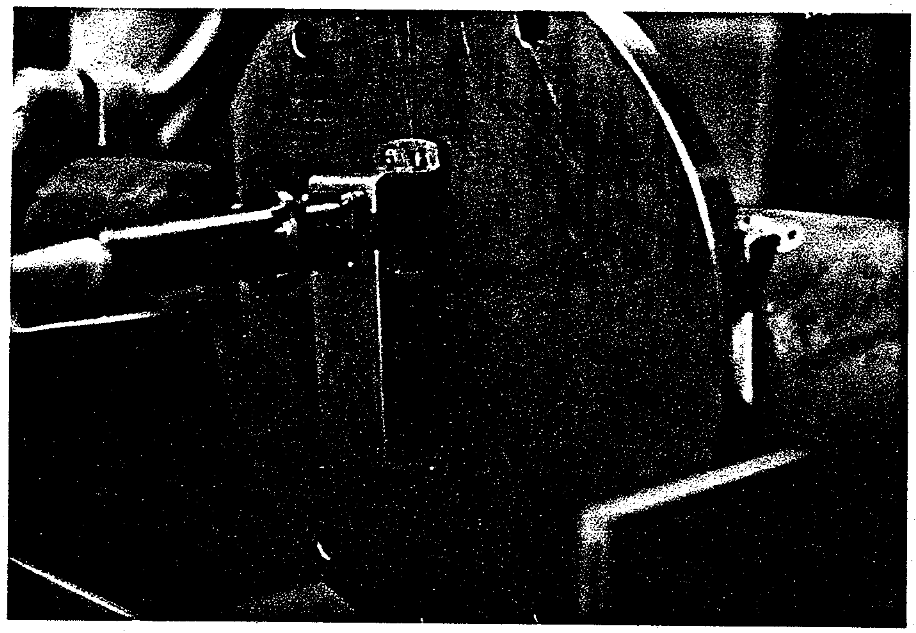

Figure 4.16 : SOLID FLANGE

Higher sensitivity to the magnetic field changes was observed for the hollow flange. It appears that the magnetic field pattern is more perturbed by the solid flange shown in Fig. 4.16.

The results of the high D.C. current calibration are shown in Fig. 4.17. The characteristic shown by a solid line was measured fast enough to avoid heating of the YIG filter by the current flowing in the line. The characteristic represented by a dashed line was obtained by gradually decreasing the current in the line. A temperature effect on the magnetic circuit of the YIG filter is evident.

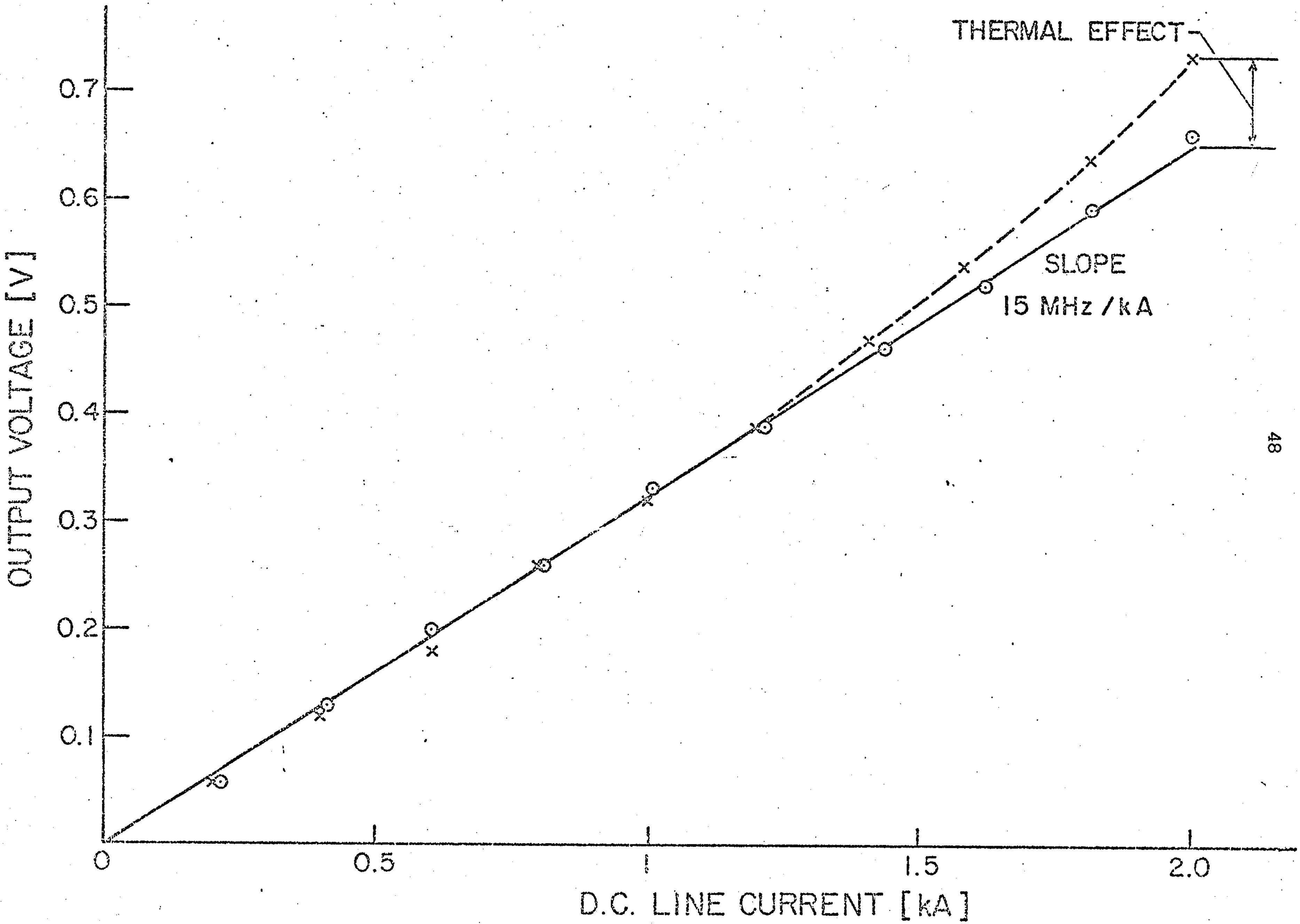

Figure 4.17 : D.C. CURRENT CALIBRATION

Chapter 5

DISCUSSION

5.1 *ATTENUATION OF THE MICROWAVE SYSTEM*

As was demonstrated in Sec. 4.2 and 4.3, the value of the open loop gain has little influence on the dynamic behaviour of the system. When return loss is greater than 10dB the system becomes nonlinear. This is an advantage since the dielectric line is subject to atmospheric interference and therefore an increase of loss may be expected.

As shown in Fig. 4.17 the available bandwidth of 400 MHz provides wide dynamic range (typically 24 kA).

5.2 *DYNAMIC BEHAVIOUR OF THE SYSTEM*

According to *MacDonald* [7], a bandwidth of 20 kHz and a rise time of 30μs were expected for the frequency lock-in system utilized in this work. The bandwidth and, therefore, the rise time depend on the open loop gain in such a way that the system has a faster response when the gain is increased. The gain of the system was increased to the highest possible value for stable operation. This was obtained by setting the return loss in the microwave system nearly to zero and by increasing the gain of the bandpass amplifier. In spite of a rise time value ten times greater than expected, the system remains faster than the existing magnetic amplifiers.

5.3 *SLEW RATE*

For small current inputs, the rise time characterizes the speed of the system. Because of nonlinear characteristic of the YIG filter, the system can become unstable when large inputs occur. In this case the slew rate becomes the most important parameter characterizing the speed of the system.

As shown in Fig. 4.6, the slew rate, on the average, is approximately 4 V/ms and is independent of the input signal frequency. This value corresponds to 12 kA/ms which is six times faster than the expected rate of an interruption of current in a typical H.D.V.C. transmission line.

5.4 *TEMPERATURE EFFECTS*

The results presented above indicate that the tracking system and the biasing magnetic circuit are influenced by the ambiant temperature. As shown in Sec. 4.9, the YIG tuned oscillator (VCO) is sensitive to temperature changes even with an internal heater operating as recommended by the manufacturer. By controlling the ambient temperature of the VCO this thermal effect can be reduced. Since the VCO is located at ground potential, temperature control does not create any particular technical problems.

Figure 4.12 shows an unexpected VCO frequency drift of 7 MHz/^{O}C, which is due to the change of the biasing magnetic field strength with ambient temperature. The main cause is the thermal expansion of the filter mount. The characteristic given in Fig. 2.6 shows that the operating point of the magnetic circuit with magnets 5 mm in diameter and 13 mm in length is 1000 Oe/mm. The thermal coefficient of Plexiglas is $5 \cdot 10^{-5}/^{\circ}C$. Since the width of the YIG filter mount is 25mm, the thermal expansion would be 0.03 mm for a temperature change of $30^{\circ}C$. For an operating point of 1000 Oe/mm thermal effect changes the biasing magnetic field by 300 Oe which, according to Fig. 4.13, corresponds to 90 MHz. This value is greater than expected because of some effects due to the misalignment of the magnets when the mount expands.

Elimination of the temperature effects on the magnetic circuit is much more difficult because the biasing magnetic circuit is placed at the high potential level where no power source is available. First of all, as can be seen in Fig. 2.6, the diameter of the magnets should be increased to obtain an operating point of the biasing magnetic field as low as possible. This would also tend to eliminate fringe effects and produce more homogeneous field in the gap. Secondly a proper design of the filter mount would eliminate the effect of the thermal expansion. By using a material with a low thermal coefficient of expansion, expansion of the mount would be minimized. Finally electronic compensation to eliminate the residual output voltage drift could be considered.

5.5 *OUTPUT STABILITY AND LINEARITY*

Under normal temperature conditions, the output stability can be evaluated. When the input was a D.C. signal the output varied approximately ±2mV about the average value. According to Fig. 4.17, this corresponds to ±6A or ±0.3% of the nominal current. The average deviation from the straight line plotted in Fig. 4.17 is 6 mV or 18 A. This deviation is due to the non-linearity of the system and the thermal effects on the biasing magnetic circuit. However, the low harmonic distortion mentioned in Sec. 4.5 implies that the system is highly linear.

5.6 *A.C. OUTPUT TEMPERATURE BEHAVIOUR*

This test (Sec. 4.8) shows that the system operates in a range of temperature from -15°C to +60°C. A decrease of the open loop gain with the temperature causes nonlinear operation of the system below -15°C.

5.7 *SENSITIVITY TO SUPPLY VOLTAGE VARIATIONS*

The result mentioned in Sec. 4.6 shows that the system is relatively insensitive to the supply voltage variations from 75 to 135 V.

5.8 *NOISE LEVEL*

The noise level and the residual 60 Hz component could be reduced by proper positioning of the electronic circuitry.

Chapter 6

CONCLUSION

The purpose of this study was to test the laboratory prototype of a new D.C. electromagnetic current transducer developed in the Department of Electrical Engineering at the University of Manitoba. Environment testing was conducted under simulated field conditions.

The results concerning the sensitivity of the system to temperature have shown that further studies are necessary to improve the accuracy of the whole system.

High linearity, fast response and wide dynamic range which are reported, confirm that the concept of the new D.C. electromagnetic transducer can prove to be a useful measurement device for H.V.D.C. power systems.

REFERENCES

[1] *Casson, W., and Lane, F.T.,* "Comparative aspects of conventional and hybride A.C. and D.C. circuits for long distance transmission", International Conference on High Voltage D.C. and/or Power Transmission, IEE London, (November, 1973), pp. 261-268.

[2] System Engineering, "Alternatives prove attractive", Electrical World, (July, 1974), pp. 72-73.

[3] *Rogers, A.T.,* "Optical Technique for measurement of current at high voltage", Proc. IEE, Vol 120, No. 2, (February, 1973), pp. 261-267.

[4] *Adamson, C., and Hiugerani, N.G.,* "New transductor-type D.C. transformer particularly applicable to H.V.D.C. systems", IEE, Vol 110, No. 4, (April, 1963), pp. 739-750.

[5] *Roschman, P.,* "YIG filters", Philips Tech. Rev., Vol. 32, No. 4, (April, 1971), pp. 322-327.

[6] *Aldecoa, T.A., and Bell, R.T.,* "YIG Applications", YIG-TEK Corporation, September, 1972.

[7] *MacDonald, A.,* M.Sc. Thesis, "A resonant frequency tracking system", Electrical Engineering Department, University of Manitoba, Winnipeg, Manitoba, 1976.

[8] *Schulten, G.,* "Applications of the dielectric line", Philips Tech. Rev., Vol. 26, No. 11/12, 1965.